archaeometry

Archaeometry ●●, ●● (2020) ●●–●● doi: 10.1111/arcm.12580

BUILDING A HIGH-RESOLUTION CHRONOLOGY AT THE MAYA ARCHAEOLOGICAL SITE OF EL PALMAR, MEXICO*

K. TSUKAMOTO†
Department of Anthropology, University of California, Riverside, CA, USA

F. TOKANAI, T. MORIYA
Center for Accelerator Mass Spectrometry, Yamagata University, Kaminoyama, Japan

and H. NASU
Faculty of Biosphere-Geosphere Science, Okayama University of Science, Okayama, Japan

This paper discusses how detailed analyses of archaeological contexts and macrobotanical remains are critical for building a high-resolution chronology in archaeological research. While the application of Bayesian modelling has improved chronology-building significantly, archaeologists have sometimes neglected different dates recovered from the same depositional layer without further scrutiny. Based on 78 radiocarbon samples, this problem is challenged by building a high-resolution chronology of the Guzmán Group, a small plaza compound of the ancient Maya city of El Palmar, Mexico. The results permit a deeper understanding of relationships between dynastic interactions and the emergence of non-royal elites in Classic Maya society.

KEYWORDS: HIGH-RESOLUTION CHRONOLOGY, BAYESIAN MODELLING, IN-DEPTH CONTEXTUAL ANALYSES, ARCHAEOBOTANY, MAYA LOWLANDS, EL PALMAR

INTRODUCTION

Since radiocarbon dating was developed in the late 1940s by Willard Libby and his team (Libby *et al*. 1949), archaeological research has hinged upon its results. At times archaeologists have been satisfied to situate their recovered materials into actual calendar years, but at other times those results have a wide range of dates preventing them from establishing a high-resolution chronology. The development of accelerator mass spectrometry (AMS) measurement techniques and new equipment such as that available at the Center of Accelerator Mass Spectrometry of Yamagata University (YU-AMS), Japan, significantly increased the precision of radiocarbon dating with tiny organic pieces (Tokanai *et al*. 2013). Despite their improvements, however, the results of multiple pieces in the same depositional layer often provide a considerable range of dates.

This issue of temporal range becomes critical for archaeologists, especially when available texts show historical events with specific dates. Maya archaeology is a case in point. Maya glyphic texts depict dynastic histories such as alliance, warfare, marriage, trade and political intervention with precise dates (Martin and Grube 2008). Increasing knowledge of Classic Maya history demands a high-resolution chronology that links historical events written on the glyphic texts with people's activities reflected in material remains. However, temporal frameworks of other archaeological remains are usually coarse, creating a considerable gap between dynastic

*Received 10 October 2019; accepted 10 May 2020
†Corresponding author: email kenichiro.tsukamoto@ucr.edu

histories based on calendrical dates and social processes reconstructed through ^{14}C and other dating methods. The application of Bayesian modelling in archaeological research is a way of mitigating this dilemma. It combines AMS ^{14}C dating with stratigraphic information and the ceramic sequence, producing refined probability distributions of calibrated dates. Using Bayesian modelling, Maya archaeologists have built a robust site chronology that has provided clues about the relationships between social processes and dynastic histories (Bachand 2008; Culleton *et al*. 2012; Munson 2012; Kennett *et al*. 2013; Aldana 2016; Inomata *et al*. 2017).

Despite the usefulness of Bayesian modelling in chronology-building, it does not fully resolve analytical uncertainties of anomalous dates recovered from the same depositional layer. When receiving two different dates from the AMS laboratory, archaeologists have neglect one of them without further contextual analyses. This is not, however, what Schiffer (1987) originally advocated in his tome on formation processes. He states that archaeologists should analyse cultural and non-cultural contexts more rigorously to identify the formation process of archaeological deposits. Following Schiffer's original statement, this paper copes with issues of

FIGURE 1 *Locations of El Palmar and other Maya sites in the Yucatan Peninsula of Mexico and Central America. [Colour figure can be viewed at wileyonlinelibrary.com]*

chronology-building by combining two methods: (1) Bayesian statistical modelling; and (2) in-depth analyses of archaeological contexts and macrobotanical remains. First, we ran Bayesian modelling for each structure based on stratigraphic relations and ceramic and architectural sequences. In this process different dates in the same depositional layer were detected. Next, temporal and spatial distributions of those different dates as well as their archaeological contexts were examined. Simultaneously, we analysed specimens recovered from the same deposit, but which produced different dates. When a specimen was too small to determine its botanical family and/or species using an optical microscope, we applied a scanning electron microscope (SEM). This analytical approach provides clues to the roles organic remains played in human activities, such as construction programmes, ritual activities, food preparation and consumption, and feasts. Finally, a high-resolution chronology of the entire plaza compound was built by correlating stratigraphic sequences among the structures. A total of 78 samples were run at YU-AMS, offering high-precision AMS radiocarbon dating with error ranges about ±20 ^{14}C years.

While building a general chronology of an entire city/polity continues to be one of the principal tasks among archaeologists, focusing on a residential compound creates a more precise temporal framework articulated with activities of a specific group of people. Identifying a residence of a specific social segment is difficult in archaeological research. Once it is discerned, however, the results provide a baseline for future comparative analyses of political organizations among different societies. We examined a small plaza compound referred as to the Guzmán Group at the site of El Palmar located in south-eastern Campeche, Mexico (Fig. 1). The Guzmán Group has an exceptional historical context. Inscriptions carved on a stairway attached to the main temple of this group refer to standard-bearers who lived in there (Tsukamoto *et al*. 2015). The texts further depict that their protagonist played an important role in dynastic interactions during the eighth century CE. By generating a high-resolution chronology, this paper assesses sociopolitical implications of standard-bearers in dynastic interactions.

METHODOLOGICAL ISSUES OF CHRONOLOGY-BUILDING IN ARCHAEOLOGICAL RESEARCH

Unlike classical statistics, the principle underlying the Bayesian approach is the incorporation of relevant prior information into the statistical analysis of data. In archaeology prior information includes stratigraphic relations and ceramic sequence. It embraces a mechanism for dealing with uncertainty and formalizing the relationship between presuppositions and conclusions to produce the refined probability (Buck *et al*. 1996, 2). Bayesian analysis is especially powerful for evaluating archaeologically stratified sequences of radiometric dates, primarily radiocarbon dates (Bachand 2008, 20). Among different programs available for the application of the Bayesian approach to chronology-building, the OxCal 4.3 program with the IntCal 13 calibration curve is of particular relevance (Bronk Ramsey 2019). Culleton *et al*. (2012, 1577, tab. 3) created a useful table that lists important OxCal commands and their associations with stratigraphic relations. We do not repeat those commands here, but a 'Phase' command is noteworthy to mention.

Archaeological research in practice usually encompasses some degree of uncertainties in stratigraphic relations when excavations take place. The Phase command incorporates these uncertainties as prior knowledge into the Bayesian statistical analysis. It loosely arranges all dates in a given time interval without constraining them in the same year or a sequence. For example, an archaeologist found two burials (A and B) intruding the latest floor of a structure. Ceramic types of offerings associated with these two burials indicate that Burials A and B were roughly contemporaneous as prior knowledge. Because the burials were intrusions, stratigraphic relations are ambiguous. A charcoal sample derived from Burial A dates to 630–670 cal. CE (95.4% at 2σ),

while that from Burial B dates to 680–720 cal. CE (95.4% at 2σ). In this case, we should use the Phase function instead of the Sequence function unless additional information about the sequence of the burials is available. Otherwise, the Sequence function forcefully orders Burial A as the earlier event than Burial B, creating an unproved historical sequence, thus two independent historical events. Yet, what should we do with two specimens found in the same depositional layer, but with different dates? The present study confronted this situation in on-floor deposits resulting from an abandonment event which we will discuss below.

Radiocarbon errors stem from cultural and non-cultural formation processes, some of which are detectable through contextual analyses. The methods used in this study are twofold: (1) analysing the spatial distribution of two or more specimens that produced different dates from the same depositional layer; and (2) the identification of wood species. Scholars have generally analysed formation processes of the archaeological record (Schiffer 1987), but do not usually

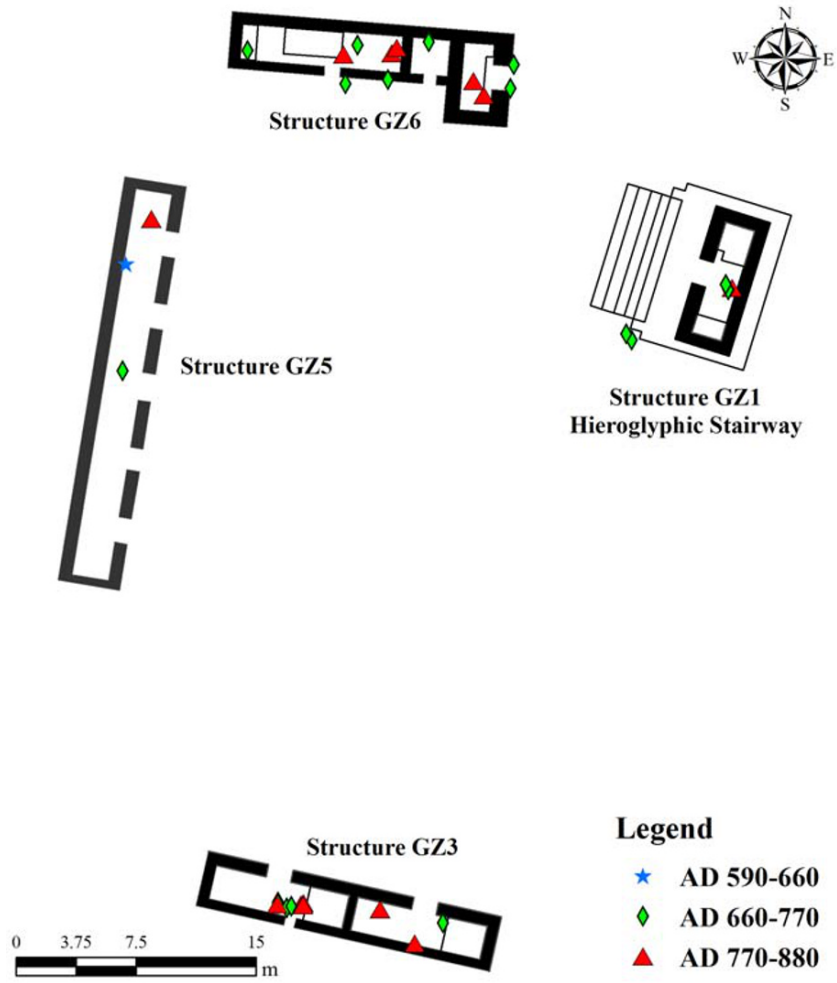

FIGURE 2 *Plan of the Guzmán Group with the distribution of radiocarbon samples. [Colour figure can be viewed at wileyonlinelibrary.com]*

illustrate the location of specimens. We documented the Universal Transverse Mercator (UTM) coordinates of each sample using a total station and analysed the spatial distribution of those samples.

We combined this contextual analysis with the identification of botanical specimens. David Lentz and his team have demonstrated the significance of identifying carbonized plant species in archaeological research (Lentz 1991; Kennett *et al*. 2013; Lentz *et al*. 2016). Although the goals of their studies are different from the present study, we find their method applicable to high-resolution chronology-building. Following their methods, we used an SEM to identify plant species. Micrographs were recorded at 50–700× magnifications, and wood types were identified through comparison with modern reference collections and the literature (Pennington and Sarukhán 2005; Lentz *et al*. 2014). This technique also helps to ascertain the degree of decay resistance in wood samples. Some hardwood species such as Chicozapote (*Manilkara zapata* L.) are more resistant to decay than edible fruit such as avocado (*Persea americana*) under the same deposit. These methods produce high-precision radioncarbon dating that fills a gap between epigraphic data of dynastic interactions and archaeological data of social processes. We realized the significance of combining AMS dating and the detection of botanical species later in the process of this study, and therefore some of the samples used for dating below did not have sizes large enough to detect their species. Nevertheless, building a high-resolution chronology with solid contextual analyses and the detection of some species permitted the articulation of the social processes that occurred at the Guzmán Group with broader dynastic interactions in the Maya lowlands.

SITUATING EL PALMAR IN THE MAYA DYNASTIC HISTORY DURING THE CLASSIC PERIOD (378–900 CE)

El Palmar consists of a civic core or the Main Group and its surrounding outlying groups (see also the additional supporting information). One of the *plazuelas* is the Guzmán Group, an outlying group located 1.3 km north of the Main Group (Fig. 2). Since 2007, Tsukamoto and Javier López Camacho have codirected the El Palmar Archaeological Project (Proyecto Arqueológico El Palmar in Spanish—PAEP) and intensively explored the Guzmán Group during four field seasons between 2010 and 2016. The Guzmán Group has a small plaza formed by a temple (Structure GZ1) and six rectangular structures (Structures GZ2–6, 9). The excavation of Structure GZ1 detected a stairway with inscriptions that depicted a history of standard-bearers (Tsukamoto *et al*. 2015; Tsukamoto and Esparza Olguín 2015).

Epigraphic and archaeological studies suggest that the El Palmar dynasty was involved in inter-polity interactions over centuries. After the 'Arrival' event in 378 CE (Stuart 2000), south-eastern Campeche, Mexico, and northern Petén, Guatemala, became arenas of dynastic upheavals (Martin and Grube 2008). The Arrival event opened with the arrival of Teotihuacan affiliates Sihyaj K'ahk' and Spearthrower Owl at Tikal. Tikal's local ruler was replaced by Spearthrower Owl's son. In 393 CE, Sihyaj K'ahk' presided over Río Azul, which is located 34 km south of El Palmar, by replacing a local ruler with a new dynastic line (Adams 1990, 34). The political alliance between Tikal and Río Azul appears to have continued at least during the Middle Classic (400–600 CE). Becan, a major polity situated 50 km north of El Palmar, experienced political turbulence between 450 and 630 CE, a time with material evidence of Teotihuacan influence. Several *plazuela* groups surrounding the site core were abandoned, while populations dispersed into isolated mounds constructed in outlying areas (Thomas 1981, 99–100). This drastic shift of settlement patterns suggests that major ideological changes occurred

at Becan during this period. A similar occurrence appears to have happened at El Palmar's Main Group, but more data are needed to assess it.

El Palmar's involvement in political interactions became more visible when the long adversary of Tikal, the Snake dynasty, intervened in south-eastern Campeche polities. A powerful Snake king, Sky Witness, exercised his authority in this region by overseeing the accession of a local ruler in 561 CE at Los Alacranes, a site 18 km south-east of El Palmar (Grube 2008, 193–195). The Snake dynasty's political campaign continued in the region after the relocation of its capital in 635 CE from Dzibanche to Calakmul, the largest Maya city 50 km west of El Palmar (Helmke and Awe 2016; Martin and García 2016). El Palmar's Stela 12 depicts the most powerful Snake dynasty's king, Yuknoom Ch'een II, who probably oversaw a royal dance of an El Palmar ruler at the second largest plaza of the Main Group between 639 and 686 CE (Esparza Olguín and Tsukamoto 2011).

The Late Classic (600–800 CE) witnessed the emergence of non-royal elites in the Maya lowlands. Numerous titled elites were depicted on stone monuments and polychrome vessels including standard-bearers (Houston and Stuart 2001; Lacadena 2008; Stuart 2010 [1992]; Jackson 2013). At El Palmar standard-bearers probably served as ambassadors for alliances between El Palmar, Copán and Calakmul in 726 CE (Tsukamoto and Esparza Olguín 2015). Inscriptions carved on the temple's stairway suggest that standard-bearers lived in the Guzmán Group over generations. The identification of this standard-bearers' residence is the first evidence of its kind in Maya archaeology (Tsukamoto *et al*. 2015). To better understand the nature of standard-bearers and their roles in dynastic interactions in Classic Maya society, PAEP explored four structures and the plaza at the Guzmán Group. Over four field seasons (2010–16) the excavations yielded a total of 120 radiocarbon samples, of which 78 were selected for AMS dating that took place at the Center for Accelerator Mass Spectrometry of Yamagata University (shown as YU-number).

The 78 samples were collected from termination rituals, fire rituals, hearths, burned features and construction fill. None of the samples was recovered from screened sediments. When possible, we chose a single large piece of charcoal to avoid creating bulk samples (Culleton *et al*. 2012, 1575). Even in the same context, we collected samples independently if they were horizontally and vertically separated by > 10 cm in an excavation unit. Two or three samples from the depositional layer were dated to increase the degree of certainty. All dates are described in Table 1. Two sigma calibrated ranges were produced by OxCal 4.3 (Bronk Ramsey 2019) with an IntCal 13 atmospheric curve (Reimer *et al*. 2013). The results represent calibration dates as 'cal. CE' or 'cal. BCE' to differentiate them from calendar years derived from epigraphic data. The calibration dates are produced in the 95.4% probability ranges (i.e., 2σ calibration range).

RESULTS

The analysis took place in three stages to build a high-resolution chronology for the Guzmán Group. First, each building's chronology was constructed independently. In this process, we carefully analysed the spatial distributions, contexts, and botanical species using the SEM. By correlating the stratigraphic relations and ceramic sequences among the structures, the second step was to build a high-resolution chronology of the entire group. Finally, historical events recorded in the group were compared with epigraphic and archaeological data from other dynasties in the Maya lowlands. Detailed information about the excavations is already published by Tsukamoto *et al*. (2015, 2018). Therefore, we briefly describe the characteristics of each building. For the

Table 1 *Results of accelerator mass spectrometry (AMS) ^{14}C dating and Bayesian models*

Laboratory no.	*Structure*	*Material*	*Context*	*$d^{13}C$ (‰)*	*Conventional ^{14}C age (BP) (yr BP ± 1σ)*	*2σ cal. range (prior) 95.4%*	*Bayesian modelled 1*	*Agreement index*	*Bayesian modelled 2*	*Agreement index*	*Ceramic phase*
YU-4081	GZ1	Charcoal	Under Floor 1, SW corner	−23.57 ± 0.25	1279 ± 20	673–770 CE	676–755 CE	93.8	691–743 CE	90.1	Chintok
YU-4101	GZ1	Charcoal	Termination ritual, GZ1-Sub 2	−28.57 ± 0.46	1474 ± 21	552–639 CE	561–644 CE	92.2	559–638 CE	104.5	Bejuco
YU-4102	GZ1	Charcoal	Termination ritual, on Floor 1 of the SW corner	−28.81 ± 0.43	1259 ± 20	675–775 CE	727–770 CE	103.5	725–758 CE	103.6	Early Xcocom
YU-4124	GZ1	Charcoal	Fire ritual, Burial 1	−28.49 ± 0.30	1286 ± 20	669–729 CE (59.0%) 737–769 CE (36.4%)	637–755 CE	88.3	690–744 CE	79.6	Chintok
YU-4125	GZ1	Charcoal	Inside the shrine, Termination ritual, on Floor 1	−28.49 ± 0.48	1205 ± 20	769–886 CE	766–875 CE	100.6	779–874 CE	108.9	Early Xcocom
YU-4127	GZ1	Charcoal	Inside the shrine, Termination ritual, on Floor 1	−27.48 ± 0.62	1258 ± 20	675–776 CE	728–775 CE	96.7	725–758 CE	103.6	Early Xcocom
YU-4640	GZ3	Charcoal	East room, Termination ritual, on Floor 1	−27.64 ± 0.35	1179 ± 20	772–884 CE (94.7%) 933–936 CE (0.7%)	774–880 CE	99.4	786–874 CE	103.4	Early Xcocom

(*Continues*)

Table 1 *(Continued)*

Laboratory no.	*Structure*	*Material*	*Context*	*$d^{13}C$ (‰)*	*Conventional ^{14}C age (BP) (yr BP ± 1σ)*	*2σ cal. range (prior) 95.4%*	*Bayesian modelled 1*	*Agreement index*	*Bayesian modelled 2*	*Agreement index*	*Ceramic phase*
YU-4641	GZ3	Charcoal	East room, Termination ritual, on Floor 1	−27.55 ± 0.35	1205 ± 20	769–886 CE	774–880 CE	99.4	786–874 CE	103.4	Early Xcocom
YU-4642	GZ3	Charcoal	West room, Termination ritual, on Floor 1	−28.93 ± 0.36	1198 ± 20	771–887 CE	774–880 CE	99.4	786–874 CE	103.4	Early Xcocom
YU-4673	GZ3	Charcoal	West room, Termination ritual, on Floor 1	−26.49 ± 0.54	1223 ± 21	695–700 CE (0.8%) 710–745 CE (18.6%) 764–884 CE (76.0%)	774–880 CE	99.4	786–874 CE	103.4	Early Xcocom
YU-4674	GZ3	Charcoal	West room, Termination ritual, on Floor 1	−23.72 ± 0.80	1215 ± 24	713–744 CE (11.2%) 765–888 CE (84.2%)	774–880 CE	99.4	786–874 CE	103.4	Early Xcocom
YU-4675	GZ3	Charcoal	West room, Floor 1 fill	−23.87 ± 0.60	1428 ± 21	592–655 CE	592–655 CE				Chintok
YU-4676	GZ3	Charcoal	Ash associated with Burial 8	−24.91 ± 0.68	1270 ± 22	678–771 CE	674–768 CE	98.1	740–770 CE	113.3	Chintok

(*Continues*)

Table 1 *(Continued)*

Laboratory no.	*Structure*	*Material*	*Context*	*$d^{13}C$ (‰)*	*Conventional ^{14}C age (BP) (yr BP ± 1σ)*	*2σ cal. range (prior) 95.4%*	*Bayesian modelled 1*	*Agreement index*	*Bayesian modelled 2*	*Agreement index*	*Ceramic phase*
YU-4677	GZ3	Charcoal	Ash associated with Burial 8	−26.40 ± 0.44	1285 ± 20	669–729 CE (58.8%) 736–769 CE (36.6%)	674–768 CE	98.1	740–770 CE	113.3	Chintok
YU-4678	GZ3	Charcoal	Ash associated with Burial 8	−25.18 ± 0.47	1295 ± 21	665–725 CE (61.8%) 738–769 CE (33.6%)	674–768 CE	98.1	740–770 CE	113.3	Chintok
YU-4680	GZ3	Charcoal	West room, Floor 3 fill	−23.90 ± 0.58	2425 ± 22	735–689 BCE (13.2%) 662–648 BCE (3.1%) 546–407 BCE (79.2%)	735–407 BCE				Chacsik
YU-4681	GZ3	Charcoal	East room, near Burial 6	−26.26 ± 0.49	1283 ± 21	670–770 CE	671–769 CE	99.1			Chintok

(*Continues*)

Table 1 *(Continued)*

Laboratory no.	*Structure*	*Material*	*Context*	*$d^{13}C$ (‰)*	*Conventional ^{14}C age (BP) (yr BP ± 1σ)*	*2σ cal. range (prior) 95.4%*	*Bayesian modelled 1*	*Agreement index*	*Bayesian modelled 2*	*Agreement index*	*Ceramic phase*
YU-4682	GZ3	Charcoal	West room, near Burial 9	−25.02 ± 0.66	1513 ± 21	433–456 CE (5.2%) 468–488 CE (5.7%) 533–606 CE (84.6%)	550–610 CE	79.2	567–625 CE	101.2	Bejuco
YU-4683	GZ3	Charcoal	West room, ash on the top of Chultun 4	−26.59 ± 0.69	1439 ± 20	585–650 CE	577–640 CE	82.2	567–625 CE	101.2	Chintok
YU-4684	GZ3	Charcoal	West room, near Burial 8	−27.37 ± 0.53	1209 ± 20	727–737 CE (3.2%) 768–885 CE (92.2%)	694–835 CE	74.8	730–809 CE	80.6	Chintok
YU-4685	GZ3	Charcoal	West room, near Burial 9	−26.94 ± 0.62	1496 ± 21	558–641 CE	555–616 CE	100	567–625 CE	101.2	Bejuco
YU-4686	GZ3	Charcoal	West room, near Burial 9	−29.53 ± 0.53	1454 ± 20	570–645 CE	573–636 CE	101.9	567–625 CE	101.2	Bejuco
YU-4687	GZ3	Charcoal	West room, near Burial 9	−26.72 ± 0.49	1477 ± 20	552–636 CE	562–627 CE	114.9	567–625 CE	101.2	Bejuco
YU-4688	GZ3	Charcoal	West room, near Burial 9	−25.53 ± 0.80	1479 ± 23	547–636 CE	560–628 CE	115	567–625 CE	101.2	Bejuco

(*Continues*)

Table 1 *(Continued)*

Laboratory no.	*Structure*	*Material*	*Context*	*$d^{13}C$ (‰)*	*Conventional ^{14}C age (BP) (yr BP ± 1σ)*	*2σ cal. range (prior) 95.4%*	*Bayesian modelled 1*	*Agreement index*	*Bayesian modelled 2*	*Agreement index*	*Ceramic phase*
YU-4689	GZ3	Charcoal	West room, near Burial 8	−27.63 ± 0.60	1288 ± 21	668–728 CE (59.7%) 737–769 CE (35.7%)	667–769 CE	98.7	741–771 CE	110.3	Chintok
YU-4690	GZ3	Charcoal	West room, Chultun 4 Fill	−24.29 ± 0.68	1477 ± 22	550–636 CE	561–629 CE	115.5	567–625 CE	101.2	Bejuco
YU-4692	GZ3	Charcoal	West room, Chultun 4 fill	−24.32 ± 0.60	1436 ± 22	583–653 CE	577–641 CE	80.6	567–625 CE	101.2	Bejuco
YU-4693	GZ3	Charcoal	West room, Chultun 4 fill	−22.98 ± 0.72	1478 ± 23	548–637 CE	565–629 CE	115.5	567–625 CE	101.2	Bejuco
YU-4694	GZ3	Charcoal	West room, Chultun 4 fill	−23.07 ± 0.65	1470 ± 22	556–641 CE	565–631 CE	116.3	567–625 CE	101.2	Bejuco
YU-4080	GZ5	Charred seed	On the bedrock platform, Termination ritual	−21.10 ± 0.33	1332 ± 20	651–710 CE (88.2%) 746–764 CE (7.2%)	650–760 CE	108.5	654–682 CE	124.3	Bejuco

(*Continues*)

Table 1 *(Continued)*

Laboratory no.	*Structure*	*Material*	*Context*	*$d^{13}C$ (‰)*	*Conventional ^{14}C age (BP) (yr BP ± 1σ)*	*2σ cal. range (prior) 95.4%*	*Bayesian modelled 1*	*Agreement index*	*Bayesian modelled 2*	*Agreement index*	*Ceramic phase*
YU-4103	GZ5	Charcoal	Floor 2 fill	−28.10 ± 0.28	1308 ± 20	660–720 CE (69.3%) 741–768 CE (26.1%)	663–765 CE	106.2	665–706 CE	126.1	Bejuco
YU-4638	GZ5	Charcoal	Room inside on Floor 1	−27.80 ± 0.35	1214 ± 20	721–740 CE (7.3%) 766–885 CE (88.1%)	710–884 CE	93.3	786–874 CE	109.8	Early Xcocom
YU-4671	GZ5	Charcoal	Room inside on Floor 1	−25.61 ± 0.43	1438 ± 20	596–663 CE	568–645 CE				Early Xcocom
YU-4672	GZ5	Charcoal	Floor 1 fill	−26.09 ± 0.49	1326 ± 21	653–712 CE (83.4%) 746–764 CE (12.0%)	653–764 CE				Chintok
YU-4679	GZ5	Charcoal	Floor 2 fill	−23.84 ± 0.49	1423 ± 21	593–656 CE (95.4%)	598–656 CE				Bejuco
YU-4691	GZ5	Charcoal	Burial 7	−26.81 ± 0.60	1410 ± 21	604–660 CE	604–660 CE				Chintok

(*Continues*)

Table 1 *(Continued)*

Laboratory no.	*Structure*	*Material*	*Context*	*$d^{13}C$ (‰)*	*Conventional ^{14}C age (BP) (yr BP ± 1σ)*	*2σ cal. range (prior) 95.4%*	*Bayesian modelled 1*	*Agreement index*	*Bayesian modelled 2*	*Agreement index*	*Ceramic phase*
YU-4078	GZ6	Charcoal	Central room, Floor 1 fill	−23.74 ± 0.28	1589 ± 20	417–537 CE	465–543 CE	110.3			Chintok
YU-4079	GZ6	Charcoal	Central room, Floor 1 fill	−21.00 ± 0.31	1357 ± 20	645–682 CE	645–679 CE	101.2			Chintok
YU-4082	GZ6	Charcoal	Central room, on Floor 2	−22.98 ± 0.36	1570 ± 20	425–541 CE	426–511 CE	106.3	433–554 CE	93.4	Sabucan
YU-4083	GZ6	Charcoal	Central room, on Floor 2	−23.92 ± 0.23	1537 ± 20	427–498 CE (48.5%) 506–581 CE (46.9%)	427–499 CE	89.2	433–554 CE	93.4	Sabucan
YU-4084	GZ6	Charcoal	Central room, Floor 5 fill	−22.51 ± 0.22	1806 ± 20	132–254 CE (92.0%) 302–315 CE (3.4%)	132–316 CE				Chacsik
YU-4085	GZ6	Charcoal	West room, Termination ritual, on Floor 1 at the edge of the south wall	−23.47 ± 0.37	1294 ± 20	666–725 CE (61.3%) 738–769 CE (34.1%)	673–769 CE	102.2	694–753 CE	93.2	Early Xcocom

(*Continues*)

Table 1 *(Continued)*

Laboratory no.	*Structure*	*Material*	*Context*	*$d^{13}C$ (‰)*	*Conventional ^{14}C age (BP) (yr BP ± 1σ)*	*2σ cal. range (prior) 95.4%*	*Bayesian modelled 1*	*Agreement index*	*Bayesian modelled 2*	*Agreement index*	*Ceramic phase*
YU-4086	GZ6	Charcoal	West room, Termination ritual, on Floor 1	−24.91 ± 0.23	1270 ± 20	680–770 CE	683–769 CE	103.2	694–753 CE	93.2	Early Xcocom
YU-4087	GZ6	Charcoal	Central room, Floor 5 fill	−19.52 ± 0.24	1821 ± 20	131–241 CE	131–241 CE				Chacsik
YU-4088	GZ6	Charcoal	Central room, Chultun 2 fill	−22.23 ± 0.30	1770 ± 20	180–185 CE (0.4%) 214–339 CE (95.0%)	238–321 CE	121.4	239–325 CE	101.9	Chacsik
YU-4089	GZ6	Charcoal	Central room, Floor 5 fill	−24.50 ± 0.28	1753 ± 20	234–345 CE	251–328 CE	111.6	255–338 CE	106.2	Chacsik
YU-4090	GZ6	Charcoal	Central room, the bottom of Chultun 2	−26.54 ± 0.42	3912 ± 21	2472–2339 BCE (93.9%) 2317–2310 BCE (1.5%)	n.a.				Chacsik
YU-4091	GZ6	Charcoal	Central room, Floor 5 fill	−28.02 ± 0.40	3869 ± 21	2462–2286 BCE	n.a.				Chacsik

(*Continues*)

Table 1 *(Continued)*

Laboratory no.	*Structure*	*Material*	*Context*	*$d^{13}C$ (‰)*	*Conventional ^{14}C age (BP) (yr BP ± 1σ)*	*2σ cal. range (prior) 95.4%*	*Bayesian modelled 1*	*Agreement index*	*Bayesian modelled 2*	*Agreement index*	*Ceramic phase*
YU-4092	GZ6	Charcoal	West room, Termination ritual, on Floor 1	−28.83 ± 0.53	1326 ± 21	653–712 CE (83.4%) 746–764 CE (12.0%)	666–764 CE	52.9			Early Xcocom
YU-4093	GZ6	Charcoal	West room, Termination ritual, Floor 1	−29.92 ± 0.44	1226 ± 20	695–701 CE (1.2%) 709–745 CE (23.1%) 764–881 CE (71.1%)	779–880 CE	87.4	779–875 CE	102.3	Early Xcocom
YU-4104	GZ6	Charcoal	East room, Termination ritual, on Floor 1	−24.31 ± 0.34	1250 ± 20	678–779 CE (89.0%) 791–805 CE (2.2%) 813–825 CE (1.4%) 840–862 CE (2.9%)	690–771 CE	102	694–753 CE	93.2	Early Xcocom
YU-4105	GZ6	Charcoal	East room, Termination ritual, on Floor 1	−27.88 ± 0.27	1256 ± 20	675–777 CE (94.7%) 793–800 CE (0.7%)	687–770 CE	101.5	694–753 CE	93.2	Early Xcocom

(*Continues*)

Table 1 *(Continued)*

Laboratory no.	*Structure*	*Material*	*Context*	*$d^{13}C$ (‰)*	*Conventional ^{14}C age (BP) (yr BP ± 1σ)*	*2σ cal. range (prior) 95.4%*	*Bayesian modelled 1*	*Agreement index*	*Bayesian modelled 2*	*Agreement index*	*Ceramic phase*
YU-4106	GZ6	Charcoal	Near Burial 2	−27.18 ± 0.19	1294 ± 20	666–725 CE (61.3%) 738–769 CE (34.1%)	673–769 CE	102.2	677–720 CE	100	Bejuco
YU-4107	GZ6	Charcoal	Near Burial 3	−28.19 ± 0.20	1201 ± 20	770–887 CE	766–847 CE	99.3	769–840 CE	104.1	Chintok
YU-4108	GZ6	Charcoal	Near Burial 3	−29.41 ± 0.25	1203 ± 20	769–887 CE	766–848 CE	100	769–840 CE	104.1	Chintok
YU-4109	GZ6	Charcoal	Near Burial 3, possible Floor 4 fill	−27.82 ± 0.23	1765 ± 20	223–338 CE	223–338 CE				Chintok
YU-4110	GZ6	Charcoal	Near Burial 3	−25.62 ± 0.20	1348 ± 20	646–689 CE	646–688 CE				Chintok
YU-4111	GZ6	Charcoal	Near Burial 3	−26.34 ± 0.22	1226 ± 20	695–701 CE (1.2%) 709–745 CE (23.1%) 764–881 CE (71.1%)	724–846 CE	112.2	769–840 CE	104.1	Chintok

(*Continues*)

Table 1 *(Continued)*

Laboratory no.	*Structure*	*Material*	*Context*	*$d^{13}C$ (‰)*	*Conventional ^{14}C age (BP) (yr BP ± 1σ)*	*2σ cal. range (prior) 95.4%*	*Bayesian modelled 1*	*Agreement index*	*Bayesian modelled 2*	*Agreement index*	*Ceramic phase*
YU-4112	GZ6	Charcoal	East room, Floor 5 fill	−28.21 ± 0.20	1789 ± 20	138–201 CE (20.1%) 206–260 CE (49.6%) 279–326 CE (25.7%)	139–326 CE				Chacsik
YU-4113	GZ6	Charcoal	West room, SW corner, Floor 4 fill	−30.89 ± 0.20	1872 ± 20	78–215 CE	78–215 CE				Chacsik
YU-4114	GZ6	Charcoal	West room, Floor 4 fill	−28.15 ± 0.20	1771 ± 20	180–185 CE (0.5%) 214–338 CE (94.9%)	238–321 CE	121.8	239–325 CE	101.9	Chacsik
YU-4115	GZ6	Charcoal	West room, Floor 4 fill	−24.85 ± 0.35	1757 ± 20	232–341 CE	238–322 CE	113	239–325 CE	101.9	Chacsik
YU-4116	GZ6	Charcoal	East room, Burial 4 fill	−27.04 ± 0.23	2009 ± 20	49 BCE–52 CE	49 BCE–51 CE				Chacsik
YU-4117	GZ6	Charcoal	Floor fill associated with Chultun 3	−28.04 ± 0.42	1771 ± 20	180–185 CE (0.5%) 214–338 CE (94.9%)	254–338 CE	97.5			Chacsik

(*Continues*)

Table 1 *(Continued)*

Laboratory no.	*Structure*	*Material*	*Context*	*$d^{13}C$ (‰)*	*Conventional ^{14}C age (BP) (yr BP ± 1σ)*	*2σ cal. range (prior) 95.4%*	*Bayesian modelled 1*	*Agreement index*	*Bayesian modelled 2*	*Agreement index*	*Ceramic phase*
YU-4118	GZ6	Charcoal	Floor fill associated with Chultun 3	−28.98 ± 0.41	1733 ± 21	246–381 CE	254–349 CE	104.3	260–378 CE	94.4	Chacsik
YU-4128	GZ6	Charcoal	East room, Termination ritual, on Floor 1	−23.80 ± 0.42	1164 ± 20	774–900 CE (81.7%) 921–950 CE (13.7%)	779–888 CE	92.4	779–875 CE	102.3	Early Xococom
YU-4129	GZ6	Charcoal	East room, Termination ritual, on Floor 1	−26.18 ± 0.53	1184 ± 20	773–891 CE	780–882 CE	103.9	779–875 CE	102.3	Early Xococom
YU-4130	GZ6	Charcoal	Central room, Floor 5 fill	−25.35 ± 0.51	1877 ± 20	74–214 CE	76–215 CE				Chacsik
YU-4131	GZ6	Charcoal	Central room, Chultun 2 fill	−23.40 ± 0.64	1763 ± 20	225–339 CE	238–322 CE	118.8	239–325 CE	101.9	Chacsik
YU-4132	GZ6	Charcoal	West Room, beneath the lateral bench, near Burial 2	−30.51 ± 0.42	1743 ± 20	240–350 CE (93.4%) 369–378 CE (2.0%)	n.a.				Bejuco
YU-4133	GZ6	Charcoal	East room, Chultun 3 fill	−23.50 ± 0.88	1748 ± 23	235–355 CE (93.0%) 367–379 CE (2.4%)	255–342 CE	109.2	260–378 CE	94.4	Chacsik

(*Continues*)

Table 1 *(Continued)*

Laboratory no.	*Structure*	*Material*	*Context*	*$d^{13}C$ (‰)*	*Conventional ^{14}C age (BP) (yr BP ± 1σ)*	*2σ cal. range (prior) 95.4%*	*Bayesian modelled 1*	*Agreement index*	*Bayesian modelled 2*	*Agreement index*	*Ceramic phase*
YU-4134	GZ6	Charcoal	East room, GZ-Sub 2 fill	−21.62 ± 0.58	1613 ± 20	393–475 CE (56.2%) 485–535 CE (39.2%)	388–462 CE	120.1	338–521 CE	112.6	Chacsik
YU-4135	GZ6	Charcoal	West room, Termination ritual, on Floor 1	−20.82 ± 0.27	1708 ± 26	253-292 CE (8.0%) 336-430 CE (87.4%)	n.a.				Early Xcocom
YU-4136	GZ6	Charcoal	West room, Termination ritual, on Floor 1	−24.66 ± 0.49	1284 ± 20	670–730 CE (58.5%) 736–770 CE (36.9%)	676–769 CE	104.5	694–753 CE	93.2	Early Xcocom
YU-4137	GZ6	Charcoal	West room, collapse	−20.49 ± 0.43	200 ± 20	1652–1684 CE (23.9%) 1736–1805 CE (50.4%) 1935 CE (21.2%)	n.a.				Early Xcocom
YU-4639	GZ6	Charcoal	East Room, GZ6-Sub 5	−25.86 ± 0.31	1775 ± 20	246–362 CE	228–319 CE	119.4	215–319 CE	111.8	Chacsik

(*Continues*)

Table 1 *(Continued)*

Laboratory no.	*Structure*	*Material*	*Context*	*$d^{13}C$ (‰)*	*Conventional ^{14}C age (BP) (yr BP ± 1σ)*	*2σ cal. range (prior) 95.4%*	*Bayesian modelled 1*	*Agreement index*	*Bayesian modelled 2*	*Agreement index*	*Ceramic phase*
YU-4695	Plaza	Charcoal	Ash inside the heath	−26.17 ± 0.55	1791 ± 24	136–260 CE (71.9%) 279–326 CE (23.5%)	144–333 CE	99	206–321 CE	126.2	Terminal Pakluum
YU-4126	Plaza A	Charcoal	Floor 6 fill	−25.97 ± 0.35	2120 ± 20	202–88 BCE (90.6%) 77–57 BCE (4.8%)	n.a.				Terminal Pakluum

results of Bayesian modelling for each structure and the identification of macrobotanical remains, see the additional supporting information.

Structure GZ1 (hieroglyphic stairway)

This is the main temple with a hieroglyphic stairway that closes the north-east end of the plaza. The inscriptions that date to its latest building in 726 CE suggest the standard-bearers resided in the Guzmán Group. Stratigraphic excavations uncovered the structure's construction episodes. Tsukamoto (2014) uncovered Burial 1 under the temple's internal floor. Numerous charcoal fragments on its capstone suggest that a fire ritual took place during a mortuary practice. Judging from the stratigraphic correlation, these two events were contemporaneous. Before the stairway, there was a substructure with a modest stairway. At the bottom of the structure, the excavation detected a termination ritual, a ritual that the Maya conducted when renewing or abandoning their building and site (Mock 1998). When abandoning, standard-bearers conducted a termination ritual again in and around the structure (Tsukamoto 2017).

Six charcoal samples were used for radiocarbon dating of this structure: (1) one from a termination ritual at the bottom of the structure; (2) one from the fire ritual associated with Burial 1; (3) one under the floor of the structure's south-west corner and another on it; and (4) two on the shrine's floor. We added the construction date of the hieroglyphic stairway, 726 CE, as a calendrical date.

The results of the Bayesian analysis show that the first termination ritual took place along with the building of GZ1-Sub 2 in cal. CE 561–644 (YU-4101) (see Figs S1 and S2 in the additional supporting information). Subsequently, GZ1-Sub 1 was built between 646 and 726 CE. In front of the structure during this time, a platform existed with a *chultun* (Chultun 1), an underground bottle-shaped chamber probably used for water catchment or storage. Standard-bearers remodelled GZ1-Sub 1 by installing the hieroglyphic stairway in 726 CE. Simultaneously, they conducted a mortuary ritual (Burial 1), depositing a male individual together with two Late Classic polychrome vessels (Tsukamoto *et al*. 2015). Burial 1 accompanied a fire ritual that dates to cal. CE 637–755 (YU-4124), which accords well with the hieroglyphic stairway's building date. YU-4081 recovered under the latest floor of the structure's south-west corner also dates to cal. CE 676–755 (see Figs S3 and S4 in the additional supporting information). The micrograph shows that this specimen was cacao (*Theobroma cacao*) or tablote (*Guazuma ulmifolia*), probably associated with feasting (Fig. 3: 1).

A problem lies in the abandonment process, but the spatial and paleobotanical analyses help to define their formation processes. Three specimens were found in the same on-floor deposit associated with a termination ritual, but are grouped into two different dates. The first date falls in cal. CE 727–775 (YU-4102, 4127) and the second in cal. CE 766–875 (YU-4125). The on-floor ceramic assemblage related to the ritual dates to the first half of the Terminal Classic (*c*.800–850 CE), including Tumba Black-on-orange and Ticul Slate. This means the first two samples were cut or carbonized earlier unless they were the centre of hardwood trunks. Excavators found YU-4102 on the floor of the Structure GZ1's south-west corner and its micrograph represents *Fabaceae* sp. (Fig. 3: 3) that was commonly used for architectural beams (Lentz and Hockaday 2009, 208; Lentz *et al*. 2014) or fuel in the Maya lowlands during this period. Although we do not preclude the possibility that it was used for fuel, people swept out the structure floor constantly and therefore this large piece hardly survived outside over a century, especially on the building floor next to the hieroglyphic stairway that faces the plaza. Rather, we assume that *Fabaceae* sp. was used for an architectural beam. During the termination ritual the beam

could have been burned and fell down together with vault stones to the outside building corner. In contrast, YU-4127 was recovered from the interior floor surface of the upper shrine. The SEM analysis identified it as pine (*Pinus* sp.) (Fig. 3: 5). A possible context is that they were parts of the building such as beams and fell down as YU-4102, or standard-bearers repeatedly conducted burning rituals inside the temple over time, accumulating pieces of charcoal. One of the Burial 1's vessels shows fire ritual scenarios inside the temple (Tsukamoto *et al*. 2015, 208, fig. 6), and we found remains of fire ritual on and under the cist (YU-4124). These lines of evidence suggest that fire rituals took place repeatedly within the temple. Finally, YU-4125 (cal. CE 766–875) was found on the shrine's floor and the SEM analysis identified it as avocado (*P. americana* or *Licaria* sp.) (Fig. 3: 4). The avocado was a common edible fruit native to Mexico (Pennington and Sarukhán 2005, 182–183). Because this plant cannot last without being carbonized, the burning and depositional events were contemporaneous. We suggest that feasting took place during the termination ritual.

Structure GZ3

It closes the south end of the plaza and consists of two rooms, each of which has an entrance and a masonry bench. Two stratigraphic excavations penetrating the west room's floor detected two previous floors and Chultun 4, which connected with the earliest floor. Excavators uncovered

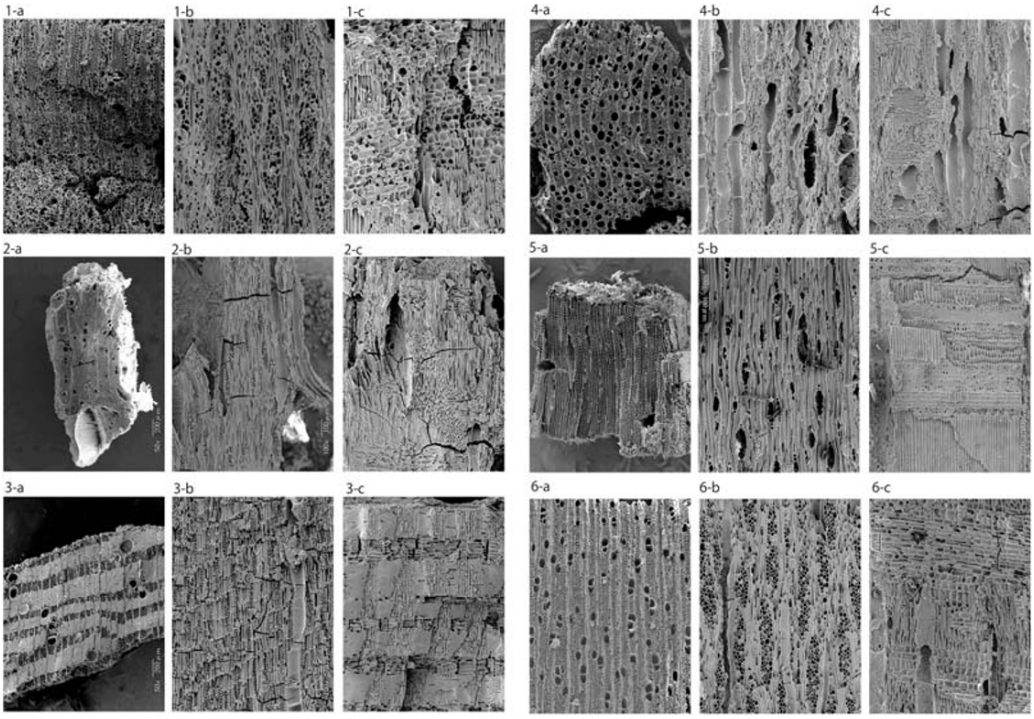

FIGURE 3 *Micrographs of paleobotanical remains: (1) Guazuma ulmifolia or Theobroma cacao (YU-4081); (2) Persea americana or Licaria sp. (YU-4085); (3) Fabaceae sp. (YU-4102); (4) P. americana or Licaria sp. (YU-4125); (5) Pinus sp. (YU-4127); (6) Malvaceae sp. (YU-4673); 'a', transversal section; 'b', radial section; and 'c', tangential section.*

four burials (Burials 6, 8–10), one in the east room and the others in the west room. People interred Burial 10 at the bottom of Chultun 4, which was filled with a midden on which a termination ritual was carried out. After the ritual, they paved floor 2, a floor that supports GZ3-Sub 1. In contrast, the excavation under the east room's floor detected only a floor. Standard-bearers deposited Burial 6 when paving the east room's latest floor. A fire ritual took place on Burial 8 that was located at the centre of the west room. After depositing Burial 8, the west room's floor was repaved. The offering of Burial 8 included a Tepeu 2 plate and a cylindrical vase (720–800 CE). Thus, the sequence in which the burials were deposited was Burial 10, then Burials 6 and 8, which were roughly contemporaneous. Finally, Burial 9 was interred when the lateral bench of the west room was added.

In order to construct a chronology of these historical events, we ran a total 23 charcoal samples recovered from Structure GZ3 and from its frontal plaza area for AMS dating: (1) one from a hearth located at the bottom of the plaza; (2) 10 samples from the midden that sealed Chultun 4; (3) one from construction fill associated with Structure GZ3-Sub 1; (4) one from construction fill associated with Structure GZ3; (5) five associated with Burial 8; and (6) five from a termination ritual as an abandonment event (see Figs S5 and S6 in the additional supporting information).

The results suggest that people dug natural marl to make a heath in front of Structure GZ3's west room by cal. CE 333 (YU-4695). A modest house (Structure GZ3-Sub 2) was built with Chultun 4. To prepare a flat surface of the house floor, they brought fill from different places that contained some ceramic vessels of the Late Preclassic (250 BCE–250 CE) and YU-4680 that dates to cal. BCE 735–407. This evidence may indicate that people lived around the Guzmán Group during the Middle Preclassic. The tiny size of YU-4680 prevented us from identifying its botanical species. Decades or centuries later, Chultun 4 was sealed with a midden and termination ritual on which Structure GZ3-Sub 1 was built by cal. CE 641. Ten specimens (YU-4682, 4683, 4685–4690, 4692–4694) found in and on the top of the *chultun* consistently date in a range from 550 to 641 CE. In cal. CE 720–770, Structure GZ3 was built along with the interment of Burials 6 and 8. Burial 8, which contained the Tepeu 2 ceramic assemblage, had two pieces of charcoal that date to cal. CE 694–835 (YU-4684) and cal. CE 667–769 (YU-4689). Unfortunately, none of these pieces had sizes large enough to define their botanical species. Nevertheless, the burial's ceramic offerings suggest that this mortuary practice took place in cal. CE 720–770. YU-4681 found near Burial 6 at the east room dates to cal. CE 671–769, suggesting it was interred together with Burial 8 at the west room, although the data do not allow us to determine which one was deposited earlier than the other exactly.

Unlike Structure GZ1, radiocarbon dates of a termination ritual at Structure GZ3 are consistent with the range of radiocarbon dates in the same on-floor deposit (see Fig. S7 in the additional supporting information). The modelled dates for all five samples (YU-4640–4674) fall in cal. CE 774–880. The SEM shows YU-4673 (cal. CE 774–880) pertains to a ceiba or majagua tree (*Malvaceae* sp.), a source of fibre (Lentz *et al*. 2014) (Fig. 3: 6), suggesting that it was part of a curtain or remains of textile owned by the inhabitant.

Structure GZ5

It closes the north-west end of the plaza. Excavations took place over two field seasons (2010–11 and 2016), exposing an administrative facility that was defined by a single long chamber with five entrances that face the plaza. Two stratigraphic excavations that penetrated the room's floor exposed five substructures. The earliest substructure (GZ5-Sub 5) was built by modifying the

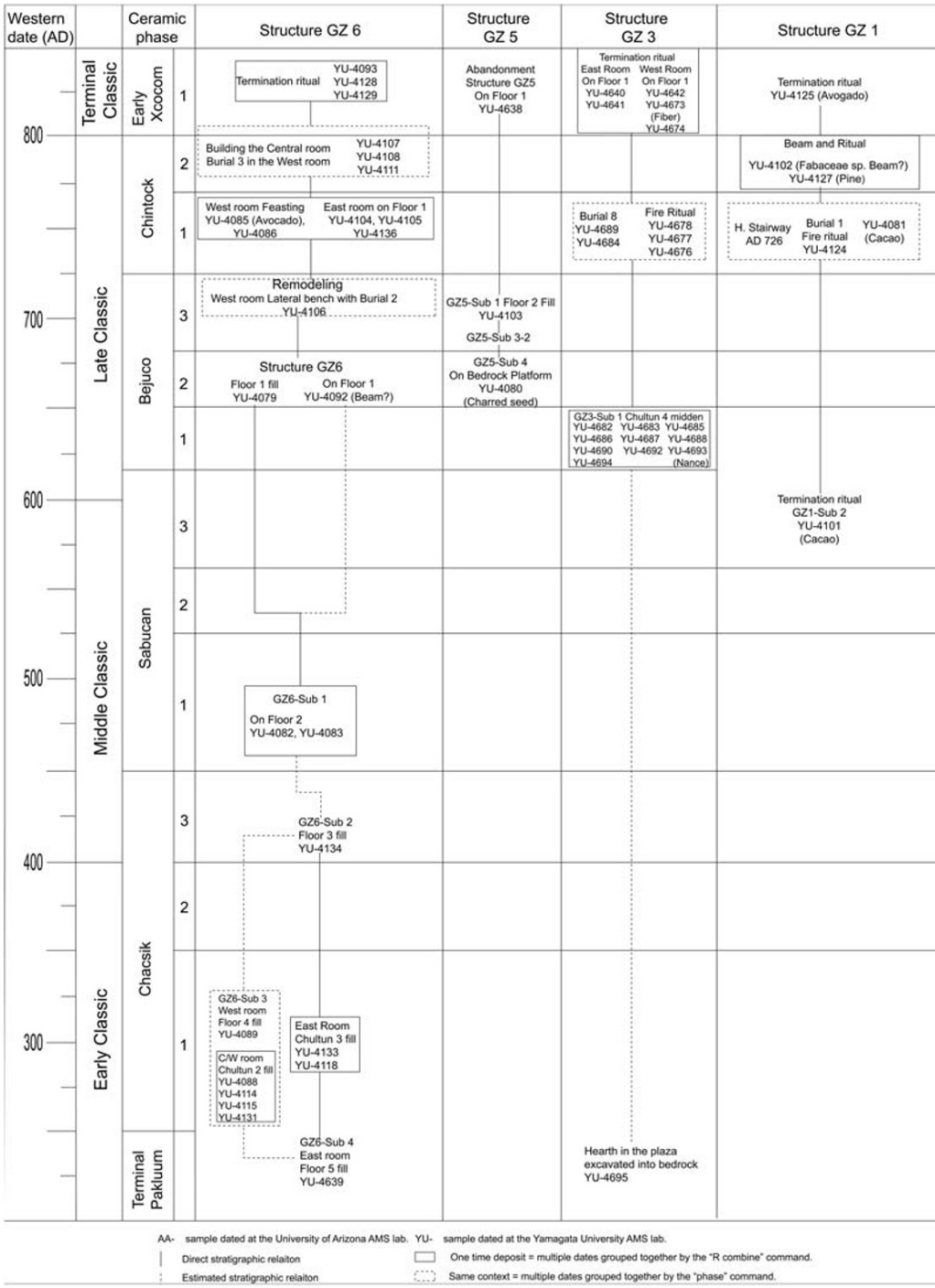

FIGURE 4 *Stratigraphic relations of radiocarbon samples with identified plant species.*

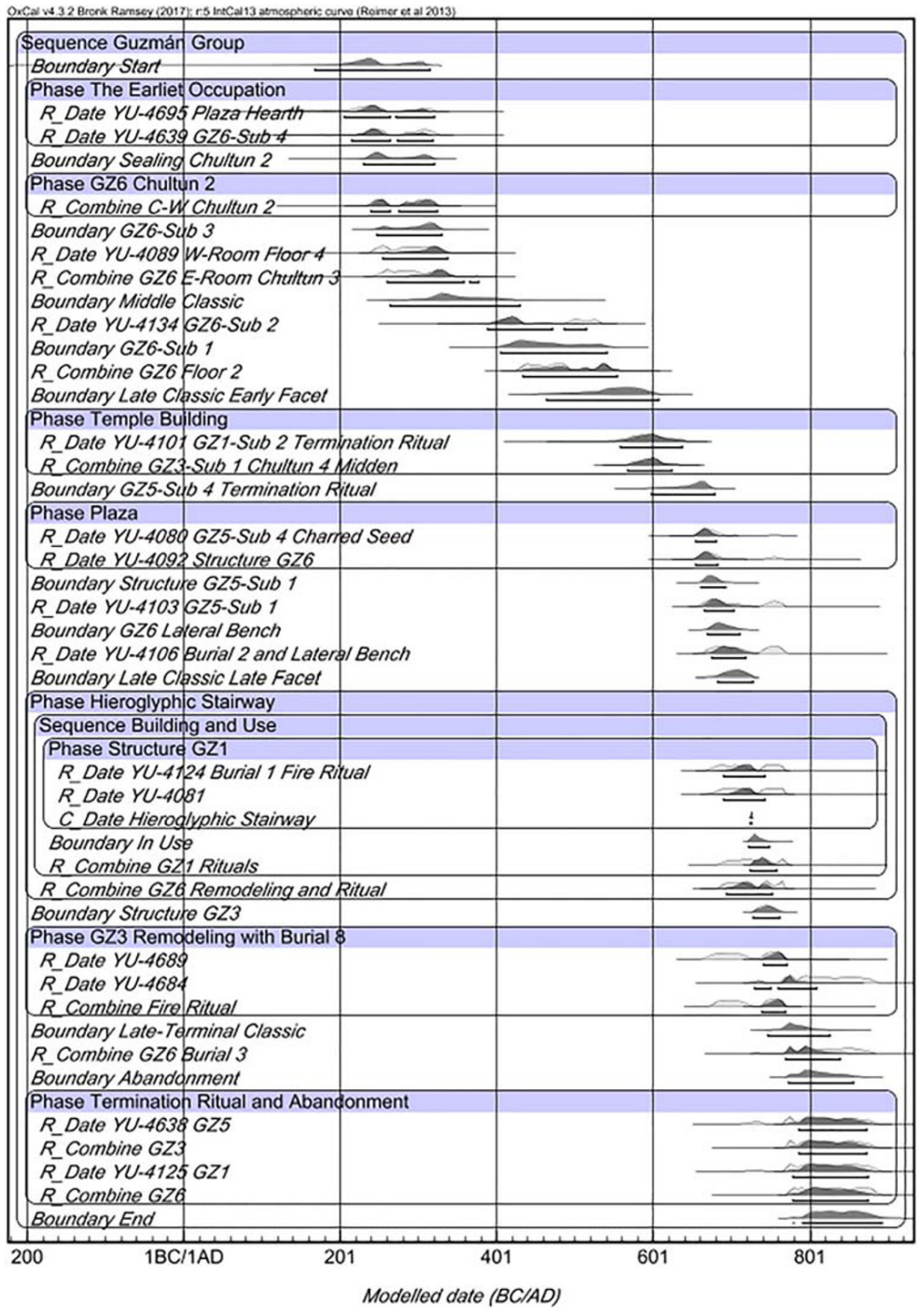

FIGURE 5 *Bayesian model 2 based on selected ^{14}C dates, stratigraphic correlations, ceramic sequences and contextual analyses using a scanning electron microscope. Outliers were excluded from the model. [Colour figure can be viewed at wileyonlinelibrary.com]*

natural marl to create a platform (Tsukamoto *et al*. 2015, 208); no archaeological remains could date this feature. However, when subsequent Structure GZ5-Sub 4 covered GZ5-Sub 5, a termination ritual was carried out on it, leaving the upper half of a red monochrome jar within which a charred seed was deposited. The jar has a transitional form that dates to *c*.600–700 CE. The excavation penetrating the latest floor yielded Burial 7 with multiple vessels. This burial was located at the centre of the chamber with rich offerings of elaborate polychrome and monochrome vessels. Unlike other structures, excavators did not identify a termination ritual as an abandonment event at Structure GZ5, suggesting its gradual abandonment.

Seven specimens were dated (see Figs S8 and S9 in the additional supporting information). The most reliable specimen was a charred seed that usually do not last more than a year in the tropical forest without being burned (YU-4080). Others include: (1) two from Structure GZ5-Sub 1's construction fill; (2) one from Structure GZ5's fill; (3) one associated with Burial 7; and (4) two on the floor of Structure GZ5 (Fig. S10). Unfortunately, several of these came from unreliable contexts such as construction fill, preventing us from dating some substructures with confidence.

Results of the Bayesian modelling suggests that GZ5-Sub 4 was built in cal. CE 650–760 based on radiocarbon dating of the charred seed (YU-4080). Because the seed does not last more than a year without being burned, the date is consonant with the time when people built GZ5-Sub 4 with the termination ritual. Furthermore, judging from the jar's transitional form the event could have happened between cal. CE 650–700. Excavators recovered two piece of charcoal from GZ5-Sub 1's construction fill (YU-4103 and 4679). Owing to the small sizes, their botanical species could not be determined. Ceramic analyses identified types of multiple periods beginning from the Late Preclassic through the Late Classic, suggesting that people levelled the GZ5-Sub 1's floor by filling debris brought from different places. The ceramic analyses predominate the first half of the Late Classic types (600–720 CE) with only a few sherds of the second half including Zacatel Cream Polychrome (720–800 CE), which partially overlaps the radiocarbon date of YU-4103 (663–760 CE). Therefore, we assume that the GZ5-Sub 1 was built in cal. CE 663–720.

The contextual and ceramic analyses suggest that Structure GZ5 was built in cal. CE 720–764. Although Burial 7 contained YU-4691 that dated to cal. CE 604–660, iconographic images on offerings suggest that this burial was deposited during the second half of the Late Classic (720–800 CE). A paleobotanical analysis identified this sample as hardwood, but it was too small to determine its species even with SEM. Nevertheless, a stratigraphic relation indicates that building of Structure GZ5 and the interment of Burial 5 were contemporaneous. YU-4672 recovered from the structure's floor fill dates to cal. CE 653–764. This date together with the offering vessels suggest that Structure GZ5 was built by cal. CE 764. These lines of evidence indicate structure's constant remodelling between cal. CE 653 and 764.

Although Structure GZ5 was gradually abandoned, a charcoal sample (YU-4638) collected on the floor surface dates to cal. CE 710–884. However, the gradual abandonment could have disturbed the archaeological context of the structure, as attested by YU-4671 (cal. CE 568–645), which was also recovered from the on-floor deposit.

Structure GZ6

This rectangular structure closes the plaza's north end. The structure received intensive excavations during the 2010–16 field seasons. The horizontal excavations exhibited three rooms with three entrances, two of which face the plaza (Tsukamoto *et al*. 2015). The west room is the most elaborate room with two masonry benches; people probably used the lateral bench for private

activities judging from its limited access and a portable incense-burner found on it (Tsukamoto *et al*. 2015, 210, fig. 9b). In contrast, the large central bench would have served for public activities such as reception and meetings. When abandoning, in and around the structure people conducted a termination ritual, partially dismantling the central bench on which they cast broken vessels, lithic tools and chert flakes.

The excavations uncovered complex construction sequences of Structure GZ6. The longest sequence was located below the east room while the shortest one was under the west room's lateral bench with Burial 2 including an offering vessel. Below the burial was a substructure whose extent remains unknown. In the east end of the west room a stratigraphic excavation exposed four floors that were penetrated by Burial 3 with a red bowl. Floor 4, the earliest floor, was associated with Chultun 2 that crosscut the central room. We found Chultun 3 under the east room that had a total of eight floors and Burial 4. These different stratigraphic sequences under the structure suggest that people originally occupied only the structure's east side, which was subsequently expanded toward the west area.

The excavations recovered a total of 50 specimens, of which 40 were used for AMS ^{14}C dating. They include: (1) 16 samples from the west room; (2) 13 from the central room; and (3) 11 from the east room. The contexts include on-floor charcoal samples associated with the termination ritual, burials and construction fill. We carefully examined the contexts and spatial distribution of these samples (see Fig. S13 in the additional supporting information).

A Bayesian model created calendrical dates of seven construction episodes and the termination ritual as an abandonment event (see Figs S11 and S12 in the additional supporting information). By 319 CE (YU-4639), Structure GZ6-Sub 4 was built in a place where the east room exists. Around that time Chultun 2 was constructed and continued to be used by cal. CE 328 (YU-4089), which is evidenced by a re-plastered floor (GZ6-Sub 3). By cal. CE 342 (YU-4117, 4118, 4133), Chultun 3 was built below the structure's east room while Chultun 2 was sealed by GZ6-Sub 3 before cal. CE 462 (YU-4134). Ceramic analyses suggest that a substructure was built under the lateral bench of the west room during this period. By cal. CE 511 (YU-4082, 4083) Structure GZ6-Sub 1 was constructed but subsequently remodelled by Structure GZ6 in cal. CE 645–679 (YU-4079, 4078). During this period, the structure consisted only of the west and east rooms, and the central room was part of the west room. None of the rooms had a masonry bench until cal. CE 673–769 (YU-4106) when Burial 2 was interred along with the lateral bench. This burial was accompanied by an Egoista Resist bowl that is a temporal marker of the early Late Classic (600–720 CE), suggesting that the bench was added in cal. CE 670–720. Decades or a century later, people interred Burial 3 in cal. CE 766–848 (YU-4107, 4108, 4110). The vessel associated with the burial, a Tinaja Red: Tinaja bowl, can further constrain this period to cal. CE 720–745. The stratigraphic relations indicate that this mortuary practice occurred together with the central room's construction. Around this time they placed the central bench in the west room. A specimen YU-4109 found near Burial 3 dates to cal. CE 223–338, which probably mixed with Floor 4 fill. Before the Terminal Classic, people deposited Burial 4 together with remodelling of the east room that included an addition to a 'U'-shaped bench. We cannot determine a specific date of Burial 4 due to the absence of reliable radiocarbon samples and datable vessel offerings.

As with Structure GZ1, several charcoal samples with different dates were recovered from on-floor deposits. From 11 specimens we collected, two samples were outliers (YU-4135 and 4137; see the additional supporting information). The remaining nine samples can be divided into two groups. The first group dates to cal. CE 666–771 (YU-4104, 4105, 4085, 4086, 4092, 4136), which accords well with the interment date of Burial 2 in the west room. The second group dates

to cal. CE 779–888 (YU-4093, 4128, 4129), which is roughly linked to the abandonment dates of the other three structures associated with termination rituals. The first group was probably related to the construction project that included an addition of the masonry benches to the west room. We discerned YU-4085 as avocado (*P. americana* or *Licaria* sp.) and excavators found it at the south edge of the west room. Ethnographic studies have demonstrated that tiny debris tends to accumulate at the corners of a room as well as the wall's edge (Hayden and Cannon 1983). YU-4085 was probably debris of feasting or other related food activities. The second group indicates the abandonment date with the termination ritual. Unfortunately, we are not sure whether the second group was associated with building beams resulting from the latest remodelling or wood materials used for the termination ritual.

UNDERSTANDING THE RELATIONSHIP BETWEEN DYNASTIC INTERACTIONS AND THE EMERGENCE OF NON-ROYAL ELITES THROUGH A HIGH-RESOLUTION CHRONOLOGY

After creating Bayesian models for each structure, we correlated stratigraphic sequences among the structures (Fig. 4). Time-sensitive botanical species helped reduce the temporal ranges of historical events including termination rituals, feasting and mortuary practices. Vessel offerings also correlated timing of construction programmes among different structures. Using the chronology of each structure as presuppositions, we created a new Bayesian model to build the high-resolution chronology of the entire group (Fig. 5; and see Fig. S14 in the additional supporting information). Except for Structure GZ5, people abandoned all the structures with termination rituals. We examined the temporal gap between *c*.670–770 and 770–880 CE in the abandonment deposits by identifying organic remains. Figure 3 shows the distribution of the two ranges of dates in the structures. The first date is probably associated with the remodelling of the plaza space in concert with the building of hieroglyphic stairway and mortuary practices, while the second corresponds to the termination rituals. Although we cannot fully preclude the possibility that the termination rituals took place at different times, ceramic assemblages found on the floors of the three structures consistently belong to the second facet of the Late Classic period with a few Terminal Classic sherds. All the on-floor radiocarbon samples of Structure GZ3 date to cal. CE 774–880, which overlaps with those from the other structures. The termination deposits contained only a few Terminal Classic sherds and the latest reliable stela at the Main Group of El Palmar is Stela 14 which dates 820 CE. These lines of evidence suggest that the termination ritual took place in cal. CE 820–875.

The high-resolution chronology of the Guzmán Group provides a baseline for understanding the relationship between dynastic interactions and the emergence of non-royal elites. Because our ceramic analyses are still ongoing, we followed the published sequence from Becan (Ball 1977), subdividing each phase into one to three sub-phases when possible.

The Arrival event seems not to have affected people in the Guzmán Group, which consisted of scattered houses with *chultunob*. The reliable date of the earliest occupation is cal. CE 206–321 when modest houses were scattered in the plaza area. Between 246 and 559 CE, only GZ6-Sub 1 was remodelled without the existence of Substructures GZ1, GZ3 and GZ5. The presence of a hearth, platform and *chultunob* on the plaza attest that people used the plaza space not for political campaigns, but for domestic activities. This implies that unlike Becan's outlying groups and El Palmar's Main Group, no major ideological change was reflected in the spatial setting of the Guzmán plaza during this period.

The transformation of the Guzmán Group occurred when the political expansion of the Snake dynasty began in south-eastern Campeche in 561 CE. Several building programmes took place at

the Guzmán Group around this time. By the end of the Bejuco 1 phase (620–640 CE), people built the temple structure GZ1-Sub 2 with a termination ritual. At Structure GZ3 they sealed the *chultun* to build Substructure GZ3-Sub 1. In Bejuco 2 (650–680 CE), when Yuknoom Ch'een II intervened at El Palmar and neighbouring dynasties, the Guzmán Group changed into a *plazuela* group. A termination ritual took place on Structure GZ5-Sub 5 in cal. CE 654–682. This substructure was remodelled three times until Structure GZ5-Sub 1 was built by 706 CE. Standard-bearers also built Structure GZ6 in Bejuco 2, but the benches and wall division between the west and the central rooms were still absent. In terms of the eastern temple, they remodelled Structure GZ1-Sub 2 with a modest stairway during Bejuco 3 (680–726 CE). Despite this major transformation, the platform located at the north-central area of the plaza still impeded to accommodate a large audience, suggesting that the plaza function was mainly for domestic use.

The Guzmán plaza became an arena of political reunion in 726 CE. Despite its defeat against Tikal in 695 CE, the Snake dynasty maintained its political authority in the Maya lowlands under the reign of Yuknoom Took' K'awiil (Martin and Grube 2008). In 726 CE when the hieroglyphic stairway was attached to Structure GZ1, the platform in front of GZ1 was partially dismantled and then buried under the new plaza surface. Standard-bearers remodelled Structures GZ3 and GZ6 with mortuary practices and fire rituals. The remains of cacao and avocado as well as large plates and bowls with heavy use-wear (Tsukamoto 2017) suggest that feasting took place repeatedly as part of political reunions. Standard-bearers were involved in dynastic alliances, especially between the Snake dynasty, Copan and El Palmar. However, epigraphic studies suggest that this alliance failed because Tikal defeated the Snake dynasty again by 736 CE. The degree of its effect on standard-bearers remain unknown. What we know is the Guzmán plaza continued to be remodelled. Structure GZ5 was probably built between cal. CE 720 and 764, serving as an administrative facility. The central room of Structure GZ6 was created and other structures' floors were repaved during Chintok 2 (770–800 CE). The Guzmán Group was abandoned with a termination ritual by 875 CE, when most Maya dynasties in the southern lowlands collapsed.

CONCLUSIONS

We suggest that political interactions among dynasties in south-eastern Campeche provoked heterogeneous urbanization processes in the El Palmar dynasty. While the Main Group experienced a major urbanization process during the Middle Classic (400–600 CE), there is no evidence of a substantial building program at the Guzmán plaza. Available data suggest that the emergence of standard-bearers at El Palmar was associated with the political intervention of the Snake dynasty in south-eastern Campeche, especially after its capital relocation to Calakmul in 635 CE. Thus, their appearance probably acted in concert with increasing interactions and demands among dynasties under the Snake dynasty's umbrella.

The Guzmán plaza became an arena of political reunion when the Snake dynasty's king, Yuknoom Took' K'awiil, attempted to encircle Tikal (Schele and Freidel 1990; Martin 1996; Tsukamoto *et al*. 2015). Standard-bearers transformed substructures of Structures GZ1, GZ3 and GZ5 and created an open space by razing a platform located in the plaza. Although the construction project within the Guzmán plaza became less active after the second defeat of the Snake dynasty with Tikal by 736 CE, this does not imply that El Palmar's standard-bearers lost political status. Structures GZ5 and GZ6 were remodelled and it is possible that the major construction project shifted to areas outside the plaza, which remain underexplored.

Chronology-building in archaeological research is crucial for understanding social processes. However, archaeologists have often faced a wide range of dates in the same depositional layer.

This paper aimed to mitigate this problem by combining Bayesian modelling, contextual analyses and the microscopic analyses of carbonized botanical remains. We found the identification of paleobotanical remains using an SEM established by Lentz (1986) and Lentz *et al*. (2014) quite useful for building a reliable high-resolution chronology. It requires a large piece of charcoal that avoids creating bulk samples. While we performed the paleobotanical analysis after AMS dating, archaeologists should integrate this analysis before running it to enhance the degree of reliability in radiocarbon samples.

ACKNOWLEDGEMENTS

The authors thank Javier López Camacho for continuous support. Travis Stanton and Jessica Munson provided thoughtful comments and suggestions on an earlier version of the manuscript. The authors also extend their gratitude to the project crews and people in Kiché Las Pailas. Archaeological research at El Palmar was generously permitted by the Mexican INAH's Consejo de Arqueología. The authors thank the University of California—Riverside and Yamagata University, the Escuela Nacional de Antropología e Historia, and the Centro INAH Campeche for institutional support. Research at El Palmar for this paper was supported by JSPS KAKENHI (grant numbers 15 J00280, 19 K13408, and 20H05141) awarded by Tsukamoto and (grant number 26101003) by Kazuo Aoyama.

REFERENCES

Aldana, G., 2016, 14C Maya long count dates: Using Bayesian modeling to develop robust site chronologies, *Archaeometry*, **58**(5), 863–80.

Adams, Richard, E. W. 1990 Archaeological Research at the Lowland Maya City of Rio Azul. *Latin American Antiquity*, **1**(1): 23–41.

Bachand, B. R., 2008, Bayesian refinement of a stratified sequence of radiometric dates from Punta de Chimino, Guatemala, *Radiocarbon*, **50**(1), 19–51.

Ball, J. W., 1977, *The archaeological ceramics of Becan, Campeche, Mexico*, Middle American Research Institute, Publication 43, Tulane University, New Orleans.

Ramsey, C. B., 2019, OxCal 4.3. In *Research Laboratory for Archaeology and the history of art*. University of Oxford, Oxford, U.K. https://c14.arch.ox.ac.uk/oxcal/OxCal.html

Buck, C. E., Cavanagh, W. G., and Litton, C. D., 1996, *Bayesian approach to interpreting archaeological data*, John Wiley & Sons, Chichester.

Culleton, B. J., Prufer, K. M., and Kennett, D. J., 2012, A Bayesian ASM ^{14}C chronology of the classic Maya Center of Uxbenká, Belize, *Journal of Arcaheological Science*, **39**, 1572–86.

Esparza Olugín, O. Q., and Tsukamoto, K., 2011, Espacios de la escenografía ritual, in *Los Mayas: Voces de piedra* (eds. A. Martínez de Velasco and M. E. Vega), 393–9, Ámbar Diseño, México City, México.

Esparza Olguín, O. Q., Tsukamoto, K., Valenzuela Campaña, L. E., and 2019, Estudio arqueológico y epigráfico del altar 10 de El palmar, Campeche, México: Un monumento maya del periodo Clásico Temprano, *Estudios de Cultura Maya*, **54**, 65–90.

Grube, Nikolai 2008 Monumentos esculpidos: epigrafía e iconografía. In Reconocimiento arqueológico en el sureste del estado de Campeche, México: 1996-2005, edited by Ivan Šprajc, pp. 177-231. Paris Monographs in America Archaeology 19. BAR International Series 1742, Oxford.

Hayden, B., and Cannon, A., 1983, Where the garbage goes: Refuse disposal in the Maya highlands, *Journal of Anthropological Archaeology*, **2**, 117–63.

Helmke, C., and Awe, J. J., 2016, Sharper than a Serpent's tooth: A tale of the Snake-head dynasty as Rocounted on Xunantunich panel 14, *The PARI Journal*, **XVII**(2), 1–22.

Houston, S. D., and Stuart, D., 2001, Peopling the classic Maya court, in *Royal Courts of the ancient Maya, volume one: Theory, comparison, and synthesis* (eds. T. Inomata and S. D. Houston), 54–83, Vol. **1**, Westview Press, Cumnor Hill.

Inomata, T., Triadan, D., MacLellan, J., Burham, M., Aoyama, K., Palomo, J. M., Yonenobu, H., Pinzón, F., and Nasu, H., 2017, High-precision radiocarbon dating of political collapse and dynastic origins at the Maya site of Ceibal, Guatemala, *Proceeding of the National Academy of Science*, **114**(6), 1293–8.

Jackson, S. E., 2013, *Politics of the Maya court: Hierarchy and change in the late classic period*, University of Oklahoma Press, Norman.

Kennett, D. J., Hajdas, I., Culleton, B. J., Belmecheri, S., Martin, S., Neff, H., Awe, J., Graham, H. V., Freeman, K. H., Lee, N., Lentz, D. L., Anselmetti, F. S., Robinson, M., Marwan, N., Southon, J., Hodell, D. A., and Haug, G. H., 2013, Correlating the ancient Maya and Modern European calendars with high-precision AMS ^{14}C dating, *Scientific Reports*, **3**(1597), 1–5.

Lacadena, A., 2008, El título Lakam: Evidencia epigráfica sobre la organización tributaria y militar interna de los reinos mayas del Clásico, *Mayab, Sociedad Española de Estudios Mayas*, **20**, 23–43.

Lentz, D. L., 1986, Archaeobotanical remains from the Hester site: The late paleo-Indian and early archaic horizons, *Midcontinental Journal of Archaeology*, **11**, 269.

Lentz, D. L., 1991, Maya diets of the rich and poor: Paleoethnobotanical evidence from Copan, *Latin American Antiquity*, **2**(3), 269–87.

Lentz, D. L., Graham, E., Vinaja, X., Slotten, V., and Jain, R., 2016, Agroforestry and ritual at the Maya Center of Lamanai, *Journal of Archaeological Science: Report*, **8**, 284–94.

Lentz, D. L., and Hockaday, B., 2009, Tikal timbers and temples: Ancient Maya agroforestry and the end of time, *Journal of Archaeological Science*, **36**(7), 1342–53.

Lentz, D. L., Lane, B., and Thompson, K., 2014, Food, farming, and Forest Management at Aguateca, in *Life and politics at the Royal Court of Aguateca: Artifacts, analytical data, and synthesis, monographs of the Aguateca archaeological project first phase, vol. 3*, 201–15, The University of Utah Press, Salt Lake City.

Libby, W., Anderson, E. C., and Arnold, J. R., 1949, Age determinations by radiocarbon content: Checks with samples of known age, *Science*, **110**, 678–80.

Martin, S., 1996, Tikal's 'star war' against Naranjo, in *The eighth Palenque round Table-1993 Vol* (eds. M. G. Robertson, M. Macri, and J. McHargue), 223–36, Pre-Columbian Art Research Institute, San Francisco.

Martin, S., and García, E. V., 2016, Polities and places: Tracing the Toponyms of the Snake dynasty, *The PARI Journal*, **17** (2), 23–33.

Martin, S., and Grube, N., 2008, *Chronicle of the Maya Kings and Queens: Deciphering the dynasties of the ancient Maya*, 2nd edn, Thames & Hudson, London.

Mock, S. B. (ed.), 1998, *The sowing and the Dawing: Termination, dedication, and transformation in the archaeological and ethnographic record of Mesoamerica*, University of New Mexico Press, Albuqurque.

Munson, Jessica 2012 Temple histories and communities of practice in early Maya Society: Archaeological investigations at Caobal, Petén, Guatemala. PhD Dissertation., School of Anthropology, The University of Arizona, Tucson.

Pennington, T. D., and Sarukhán, J., 2005, *Árboles tropicales de México: Manual Para la identificación de las principales especies. Dirección general de Publicaciones y Fomento editorial*, UNAM-Foundo de Cultura Económica, Mexico.

Reimer, P. J., Bard, E., Alex, B., Warren Beck, J., Blackwell, P. G., Ramsey, C. B., Buck, C. E., Cheng, H., Edwards, R. L., Friedrich, M., Grootes, P. M., Guilderson, T. P., Haflidason, H., Hajdas, I., Hatté, C., Heaton, T. J., Hoffmann, D. L., Hogg, A. G., Hughen, K. A., Kaiser, K. F., Kromer, B., Manning, S. W., Niu, M., Reimer, R. W., Richards, D. A., Scott, E. M., Southon, J. R., Staff, R. A., Turney, C. S. M., and van der Plicht, J., 2013, INTCAL13 and Marine13 radiocarbon age calibration curves 0–50,000 years Cal BP, *Radiocarbon*, **55**(4), 1869–87.

Schele, L., and Freidel, D., 1990, *A Forest of kings: The untold story of the ancient Maya*, Quill William Morrow, New York.

Schiffer, M. B., 1987, *Formation processes of the archaeological record. University of new Mexico Press*, Albuquerque, NM.

Stuart, D., 2000, 'The arrival of strangers': Teotihuacan and Tollan in classic Maya history, in *Mesoamerica's classic heritage: From Teotihuacan to the Aztecs* (eds. D. Carrasco, L. Jones, and S. Sessions), 465–513, Colorado University Press, Niwot, CO.

Stuart, D., 2010, [1992] the Lakam sign, in *The Lakam logogram*, Maya Decipherment: A Weblog on the Ancient Maya Script. http://decipherment.wordpress.com/2010/03/08/the-lakam-logogram/

Thomas, Prentice M., Jr. 1981, *Prehistoric Maya Settlement Patterns at Becan, Campeche, Mexico*. Publication 45. Middle American Research Institute, Tulane University, New Orleans.

Tokanai, Fuyuki, Kazuhiro Kato, Minoru Anshita, Hirohisa Sakurai, Akihito Izumi, Teiko Toyoguchi, Takeshi Kobayashi, Hiroko Miyahara and Motonari Ohyama 2013 Present Status of YU-AMS System. *Radiocarbon* **55**(2-3): 251–259.

Tsukamoto, K., 2014, Multiple identities on the plazas: The classic Maya Center of El palmar, Mexico, in *Mesoamerican plazas: Arenas of community and power* (eds. K. Tsukamoto and T. Inomata), 50–67, The University of Arizona Press, Tucson.

Tsukamoto, K., 2017, Reverential abandonment: A termination ritual at the ancient Maya polity of El palmar, *Antiquity*, **91**(360), 1630–46.

Tsukamoto, K., Camacho, J. L., Valenzuela, L. E. C., Kotegawa, H., and Esparza Olguín, O. Q., 2015, Political interactions among social actors: Spatial Organization at the Classic Maya Polity of El palmar, *Campeche, Mexico Latin American Antiquity*, **26**, 200–20.

Tsukamoto, K., and Olguín, O. E., 2015, Ajpach' Waal: The hieroglyphic stairway at the Guzmán Group of El Palmar, Campeche, Mexico, in *Maya archaeology* (eds. C. Golden, S. Houston, and J. Skidmore), 30–55, Precolumbian Mesoweb Press, San Francisco.

Tsukamoto, K., Valenzuela, L. E. C., Pesina, X. S. C., Gutiérrez, R. J. Z., Hernández, D. M. R., Hernández, M. G., Kotegawa, H., and Camacho, J. L., 2018, Proyecto Arqueológico El palmar en Campeche, México: Resultados de la Temporada de campo 2016, in *Simposio de Investigaciones Arqueológicas en Guatemala*, 31, Vol. **2017**.

SUPPORTING INFORMATION

Additional supporting information may be found online in the Supporting Information section at the end of the article.

Data S1. Supporting Information

Supplementary Material

El Palmar Archaeological Project (Proyecto Arqueológico El Palmar in Spanish, hereinafter PAEP) aims to understand the relationships between urbanization processes and sociopolitical organizations in the Maya lowlands. The PAEP has carried out surface surveys, airborne LiDAR mapping, horizontal and stratigraphic excavations, and artifactual analyses. The surface surveys recorded monumental structures with 35 stelae and 14 altars at the Main Group. Although epigraphic studies of these monuments are still in process, current data show that El Palmar had a dynasty with successive rulers at least from AD 554 until 820 (Esparza Olguín, et al. 2019). Stratigraphic excavations suggest that the Main Group was occupied from the Late Preclassic period (300 BC-AD 250) until the Terminal Classic period (AD 800-900), with rapid urbanization occurring during the Middle Classic period (AD 400-600). During the urbanization process substantial plazas were constructed at the Main Group (Tsukamoto 2014). Recent airborne LiDAR (Light Detection and Ranging) mapping that covered 94 km^2 exhibits over 500 *plazuela* groups (i.e. a plaza compound surrounding the civic-core) around the Main Group.

The chronology of the Guzmán Group, an outlying group located 1.3 km north of the Main Group was built based on two stages of Bayesian modeling. First, a chronology of each structure was created through Oxcal 4.3. During this process, we analyzed contexts and spatial distributions of samples, through which samples with different dates in the same depositional layer were detected. After building chronologies of four structures, in the second stage we correlated stratigraphic relations and ceramic sequences among the structures that resulted in creating Harris Matrix (see Figure 3 in the main text). In this process we combined some samples that have the same context by using the “Combine” command.

The paleobotanical analysis is a critical process in building a high-resolution chronology. Unfortunately, we realized it after finishing the AMS radiocarbon dating and therefore many samples had already been destroyed when we attempted to identify their botanical species. Table S1 is the list of samples which we could identify either family or species name, or both. Despite the small number of identified specimens, the results were extremely helpful for refining chronology building through contextual analyses. In future research we recommend that scholars to identify botanical species through a scanning electron microscope (SEM).

Table S1. Paleobotanical Species

Lab No.	Structure	Family name	Species name	Common name
YU-4101	GZ1	Sterculiaceae	*Guazuma ulmifolia* or *Theobroma cacao*	Tablote or Cacao
YU-4693	GZ6	Malpighiaceae	*Brysonima* sp.	Nance
YU-4081	GZ1	Sterculiaceae	*Guazuma ulmifolia* or *Theobroma cacao*	Tablote or Cacao
YU-4102	GZ1	Fabaceae	Fabaceae sp.	
YU-4127	GZ1	Pinaceae	*Pinus* sp.	Pino
YU-4085	GZ6	Lauraceae	*Persea americana* or *Licaria* sp.	Aguacate or Aguacatillo ?
YU-4673	GZ3	Malvaceae	Malvaceae sp.	Ceiba or Majagua?
YU-4125	GZ1	Lauraceae	*Persea americana* or *Licaria* sp.	Aguacate or Aguacatillo ?

Structure GZ1

The excavations yielded a total of 22 samples, of which six samples were used for radiocarbon dating.

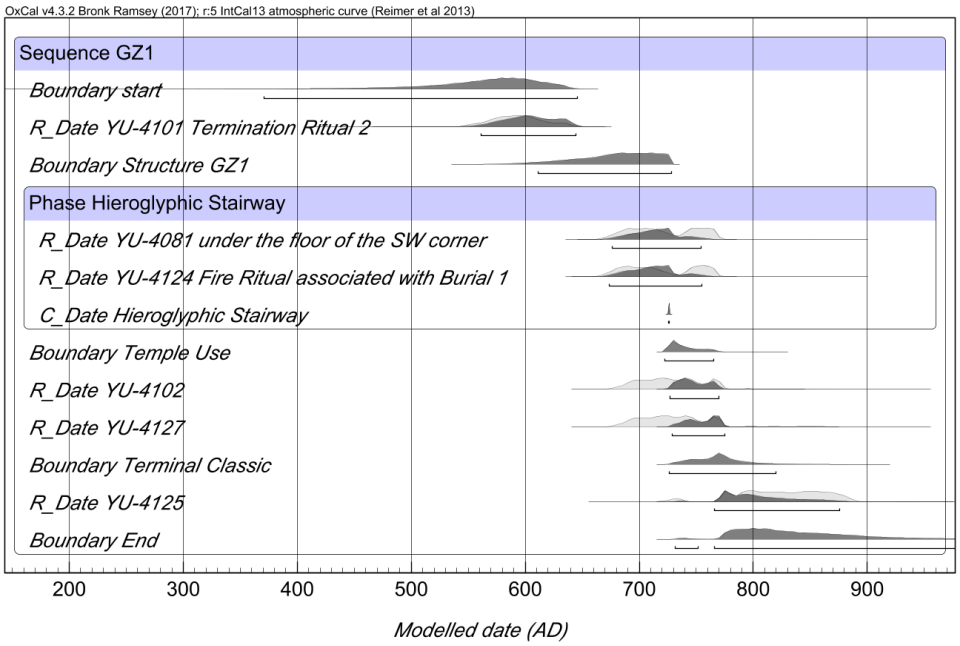

Figure S1. Bayesian-modeled radiocarbon dates of Structure GZ1.

CODE

```
Plot()
 {
  Sequence("GZ1")
  {
   Boundary("start");
   R_Date("YU-4101 Termination Ritual 2", 1474, 21);
   Boundary("Temple");
   Phase("Temple Building")
   {
    R_Date("YU-4081 under the floor of the SW corner", 1279, 20);
    R_Date("YU-4124 Fire Ritual associated with Burial 1", 1286, 20);
    C_Date("Hieroglyphic Staircase", 726, 0);
```

```
};
Boundary("Temple Use");
R_Date("YU-4102", 1259, 20);
R_Date("YU-4127", 1258, 20);
Boundary("Terminal Classic");
R_Date("YU-4125", 1205, 20);
Boundary("End");
};
};
```

Figure S2. Oxcal code for Bayesian modeling of Structure GZ1.

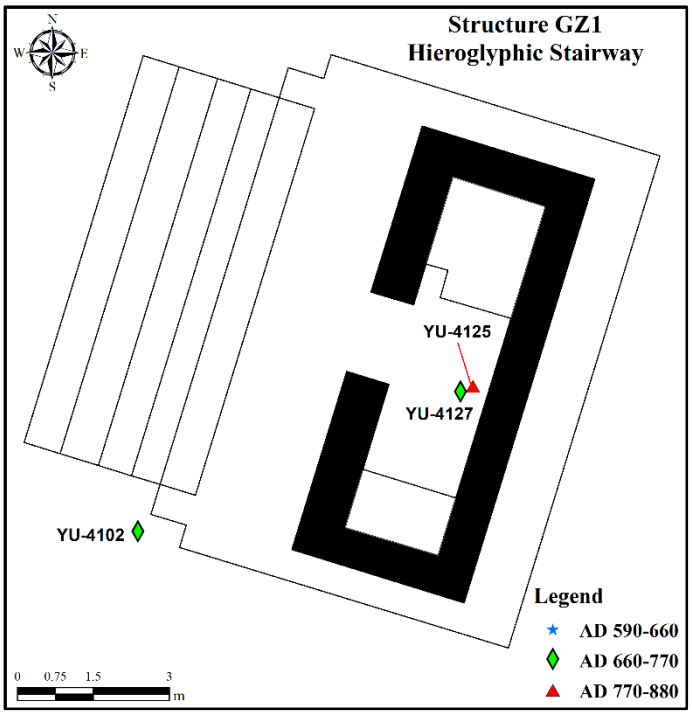

Figure S3. The distribution of on-floor radiocarbon samples associated with a termination ritual at Structure GZ1.

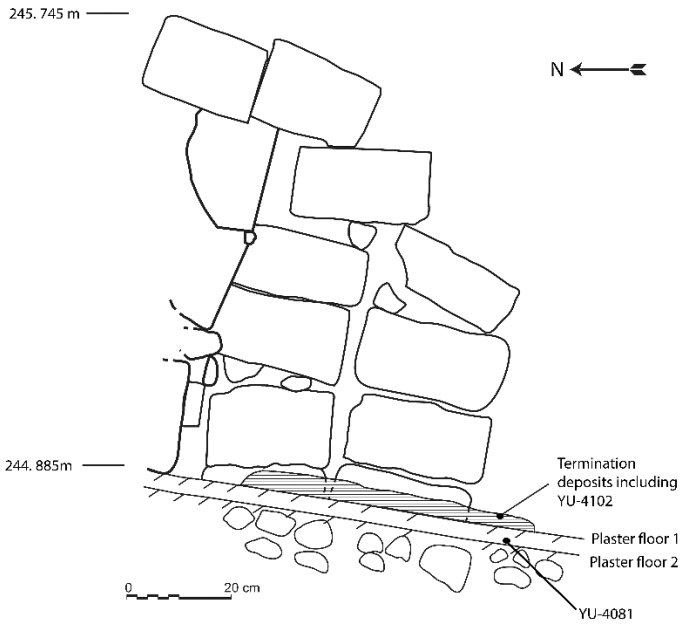

Figure S4. The profile of Structure GZ1's southwest corner with the location of specimens YU-4102 and 4081.

Structure GZ3

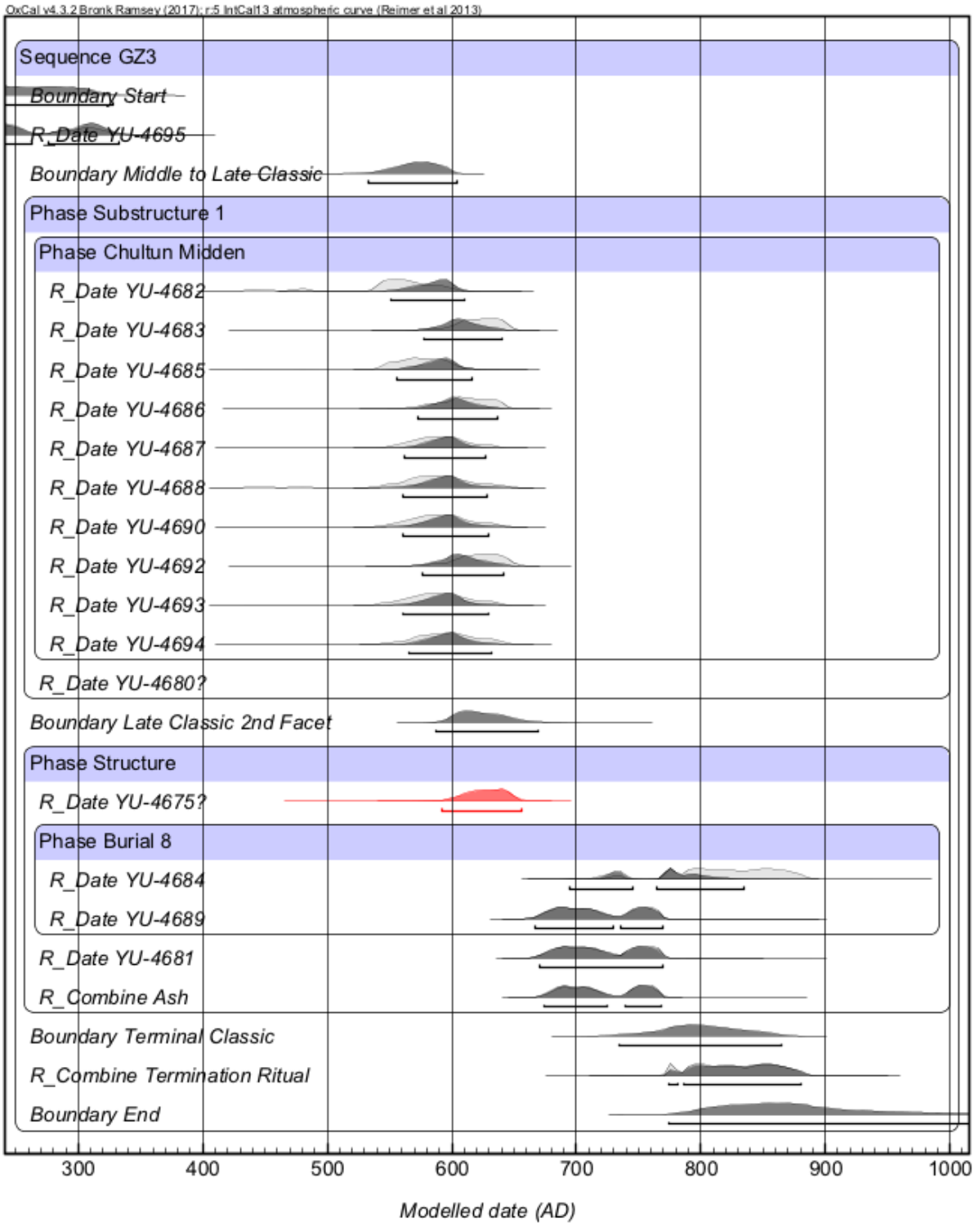

Figure S5. Bayesian-modeled radiocarbon dates of Structure GZ3.

CODE

```
Plot()
 {
  Sequence("GZ3")
  {
   Boundary("Start");
   R_Date("YU-4695", 1791, 24);
   Boundary("Middle to Late Classic");
   Phase("Substructure 1")
   {
    Phase("Chultun Midden")
    {
     R_Date("YU-4682", 1513, 21);
     R_Date("YU-4683", 1439, 20);
     R_Date("YU-4685", 1496, 21);
     R_Date("YU-4686", 1454, 20);
     R_Date("YU-4687", 1477, 20);
     R_Date("YU-4688", 1479, 23);
     R_Date("YU-4690", 1477, 22);
     R_Date("YU-4692", 1436, 22);
     R_Date("YU-4693", 1478, 23);
     R_Date("YU-4694", 1470, 22);
    };
    R_Date("YU-4680", 2425, 22)
    {
     Outlier(color="Red");
    };
   };
   Boundary("Late Classic 2nd Facet");
```

```
Phase("Structure")
{
 R_Date("YU-4675", 1428, 21)
 {
  Outlier(color="Red");
 };
 Phase("Burial 8")
 {
  R_Date("YU-4684", 1209, 20);
  R_Date("YU-4689", 1288, 21);
 };
 R_Date("YU-4681", 1283, 21);
 R_Combine("Ash")
 {
  R_Date("YU-4676", 1270, 22);
  R_Date("YU-4677", 1285, 20);
  R_Date("YU-4678", 1295, 21);
 };
};
Boundary("Terminal Classic");
R_Combine("Termination Ritual")
{
 R_Date("YU-4640", 1179, 20);
 R_Date("YU-4641", 1205, 20);
 R_Date("YU-4642", 1198, 20);
 R_Date("YU-4673", 1223, 21);
 R_Date("YU-4674", 1215, 24);
};
Boundary("End");
};
```

};

Figure S6. Oxcal code for Bayesian modeling of Structure GZ3.

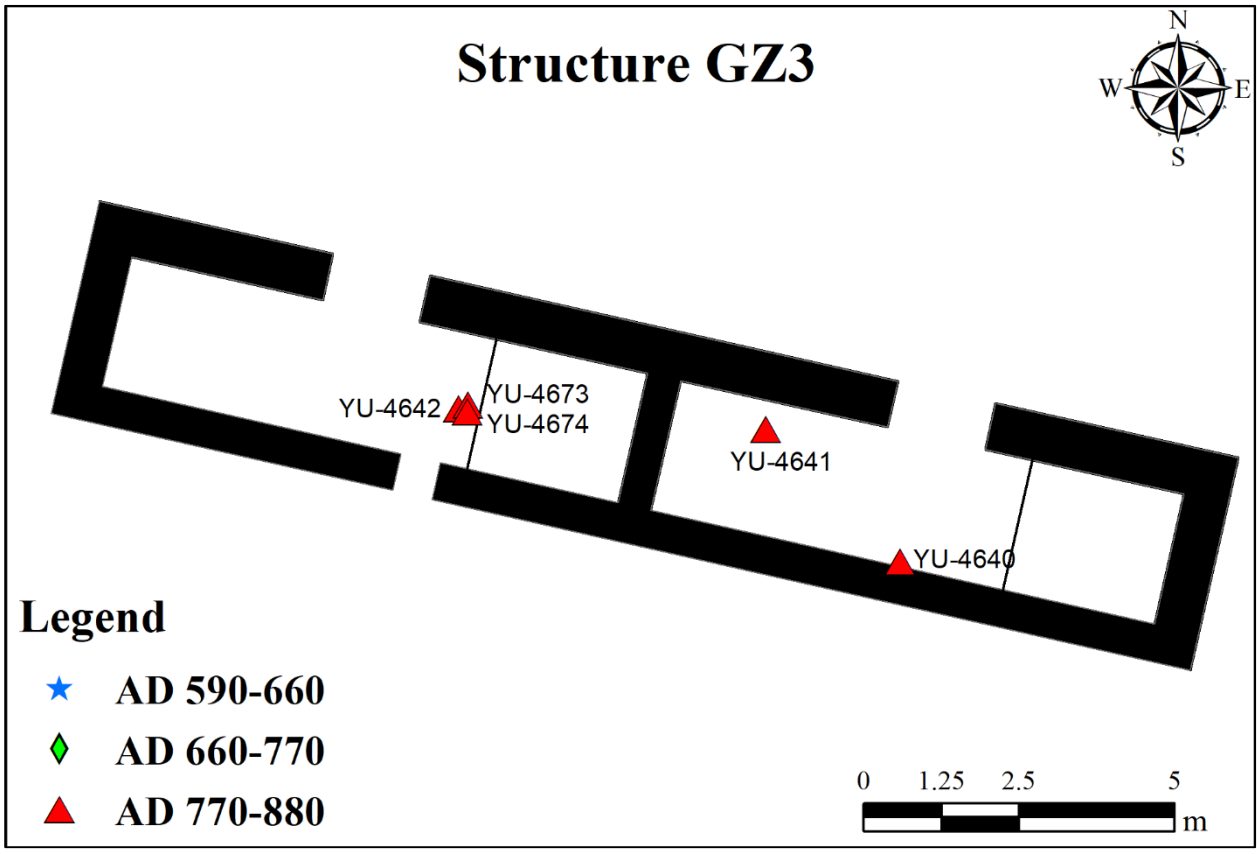

Figure S7. The distribution of on-floor radiocarbon samples associated with a termination ritual at Structure GZ3.

Structure GZ5

We recovered a total of 27 specimens, of which seven were relatively reliable and used for AMS dating.

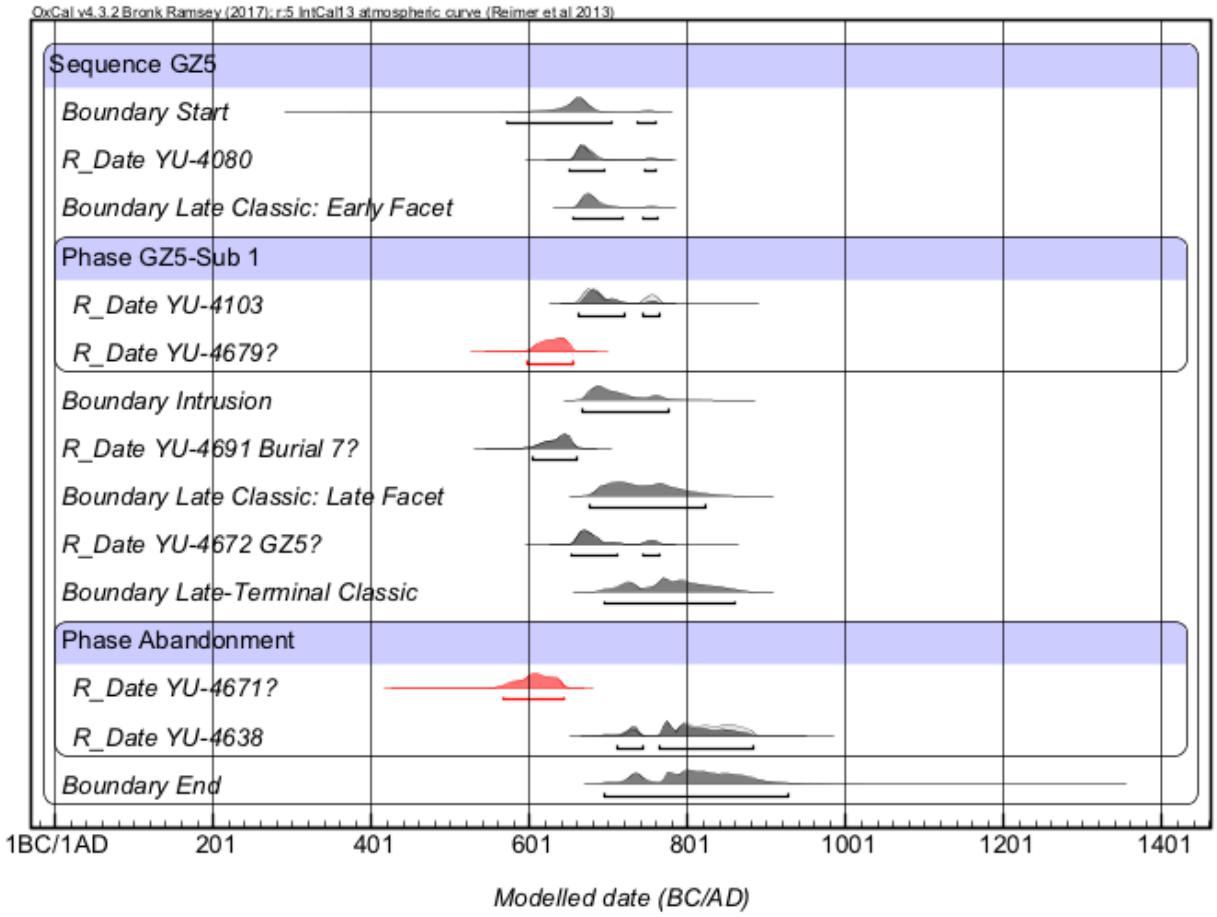

Figure S8. Bayesian-modeled radiocarbon dates of Structure GZ5.

CODE

```
Plot()
 {
  Sequence("GZ5")
  {
```

```
Boundary("Start");
R_Date("YU-4080", 1332, 20);
Boundary("Late Classic: Early Facet");
Phase("GZ5-Sub 1")
{
 R_Date("YU-4103", 1308, 20);
 R_Date("YU-4679", 1423, 21)
 {
  Outlier(color="Red");
 };
};
Boundary("Intrusion");
R_Date("YU-4691 Burial 7", 1410, 21)
{
 Outlier("Old wood");
};
Boundary("Late Classic: Late Facet");
R_Date("YU-4672 GZ5", 1326, 21)
{
 Outlier("Old wood");
};
Boundary("Late-Terminal Classic");
Phase("Abandonment")
{
 R_Date("YU-4671", 1456, 21)
 {
  Outlier(color="Red");
 };
 R_Date("YU-4638", 1214, 20);
};
```

```
 Boundary("End");
 };
};
```

Figure S9. Oxcal code for Bayesian modeling of Structure GZ5.

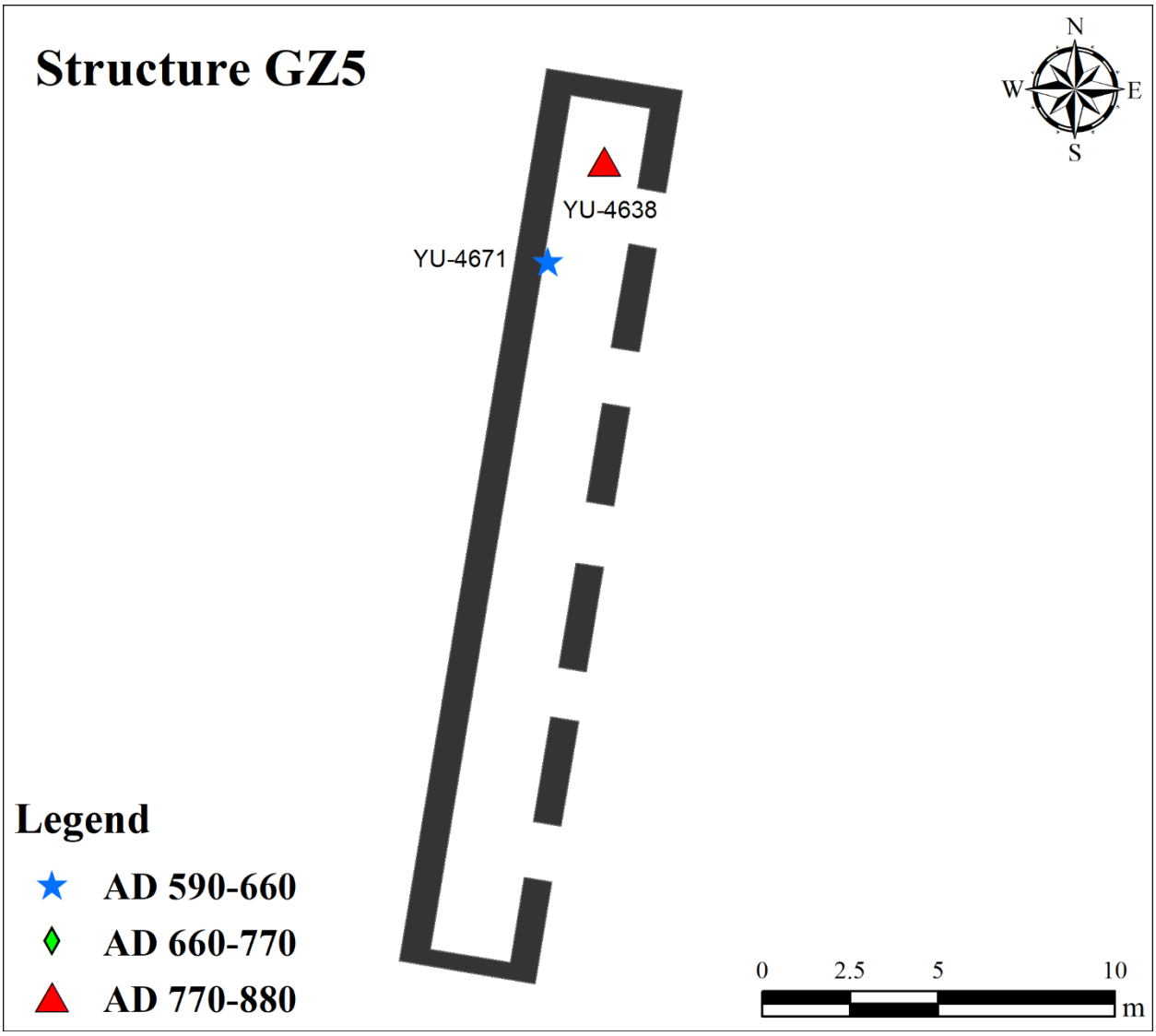

Figure S10. The distribution of on-floor radiocarbon samples associated with a termination ritual at Structure GZ5.

Structure GZ6

There are two problematic samples in the abandonment process of Structure GZ6. The specimen YU-4135, which dates to cal AD 253-430, was found on a burned floor surface of the west room. Because the piece was too small to identify its botanical species, we could not do further contextual analyses. The second one YU-4137, which dates to cal AD1662-1930, also did not contain the size enough to determine its species. Based on the modern date, however, we suggest that this was intruded by modern cultural or non-cultural formation processes.

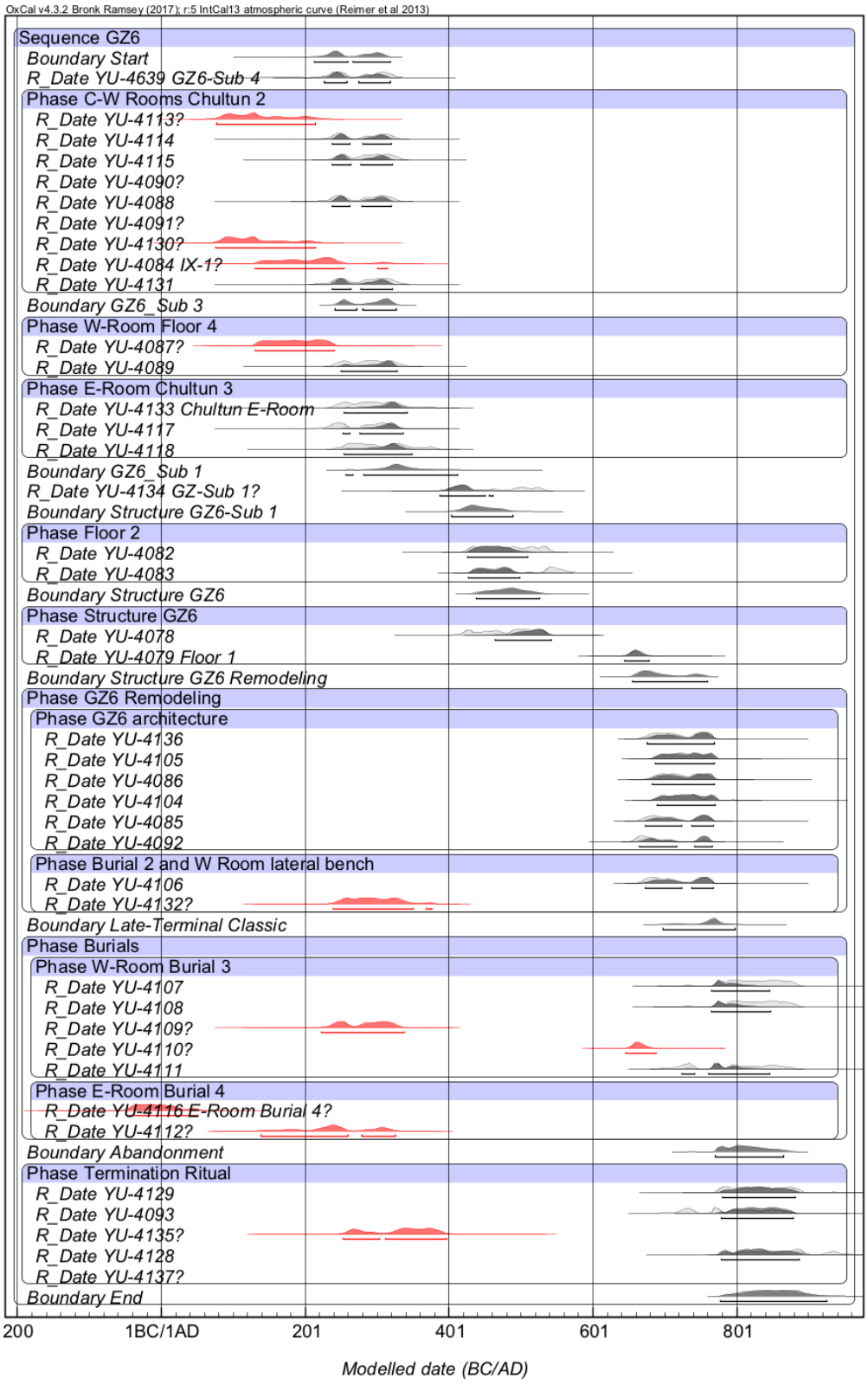

Figure S11. Bayesian-modeled radiocarbon dates of Structure GZ6.

CODE

```
Plot()
 {
  Sequence("GZ6")
  {
   Boundary(Start);
   R_Date("YU-4639 GZ6-Sub 4", 1775, 20);
   Phase("C-W Rooms Chultun 2")
   {
    R_Date("YU-4113", 1872, 20)
    {
     Outlier(color="Red");
    };
    R_Date("YU-4114", 1771, 20);
    R_Date("YU-4115", 1757, 20);
    R_Date("YU-4090", 3912, 21)
    {
     Outlier(color="Red");
    };
    R_Date("YU-4088", 1770, 20);
    R_Date("YU-4091", 3869, 21)
    {
     Outlier(color="Red");
    };
    R_Date("YU-4130", 1875, 20)
    {
     Outlier(color="Red");
    };
    R_Date("YU-4084 IX-1", 1806, 20)
    {
```

```
 Outlier(color="Red");
};
R_Date("YU-4131", 1765, 20);
};
Boundary("GZ6_Sub 3");
Phase("W-Room Floor 4")
{
R_Date("YU-4087", 1821, 20)
{
 Outlier(color="Red");
};
R_Date("YU-4089", 1753, 20);
};
Phase("E-Room Chultun 3")
{
R_Date("YU-4133 Chultun E-Room", 1748, 23);
R_Date("YU-4117", 1771, 20);
R_Date("YU-4118", 1733, 21);
};
Boundary("GZ6_Sub 1");
R_Date("YU-4134 GZ-Sub 1?", 1613, 20);
Boundary("Structure GZ6-Sub 1");
Phase("Floor 2")
{
R_Date("YU-4082", 1570, 20)
{
};
R_Date("YU-4083", 1537, 20)
{
};
```

```
};
Boundary("Structure GZ6");
Phase("Structure GZ6")
{
 R_Date("YU-4078", 1589, 20)
 {
 };
 R_Date("YU-4079 Floor 1", 1355, 20);
};
Boundary("Structure GZ6 Remodeling");
Phase("GZ6 Remodeling")
{
 Phase("GZ6 architecture")
 {
  R_Date("YU-4136", 1284, 20);
  R_Date("YU-4105", 1256, 20);
  R_Date("YU-4086", 1270, 20);
  R_Date("YU-4104", 1250, 20);
  R_Date("YU-4085", 1294, 20);
  R_Date("YU-4092", 1326, 21);
 };
 Phase("Burial 2 and W Room lateral bench")
 {
  R_Date("YU-4106", 1294, 20);
  R_Date("YU-4132", 1743, 20)
  {
   Outlier(color="Red");
  };
 };
};
```

```
Boundary("Late-Terminal Classic");
Phase("Burials")
{
 Phase("W-Room Burial 3")
 {
  R_Date("YU-4107", 1201, 20);
  R_Date("YU-4108", 1203, 20);
  R_Date("YU-4109", 1765, 20)
  {
   Outlier(color="Red");
  };
  R_Date("YU-4110", 1348, 20)
  {
   Outlier(color="Red");
  };
  R_Date("YU-4111", 1226, 20);
 };
 Phase("E-Room Burial 4")
 {
  R_Date("YU-4116 E-Room Burial 4", 2009, 20)
  {
   Outlier(color="Red");
  };
  R_Date("YU-4112", 1789, 20)
  {
   Outlier(color="Red");
  };
 };
};
Boundary("Abandonment");
```

```
 Phase("Termination Ritual")
 {
  R_Date("YU-4129", 1184, 20);
  R_Date("YU-4093", 1226, 20);
  R_Date("YU-4135", 1708, 26)
  {
   Outlier(color="Red");
  };
  R_Date("YU-4128", 1164, 20);
  R_Date("YU-4137", 200, 20)
  {
   Outlier(color="Red");
  };
 };
 Boundary("End");
};
};
```

Figure S12. Oxcal code for Bayesian modeling of Structure GZ6.

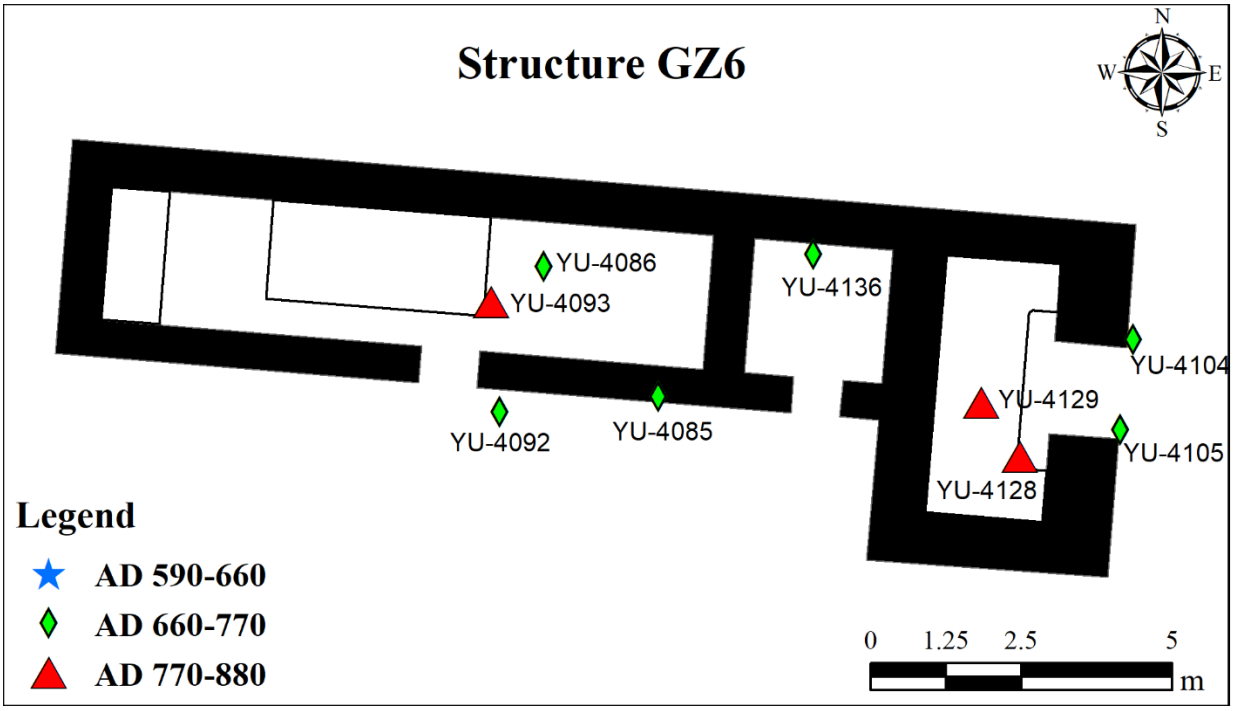

Figure S13. The distribution of on-floor radiocarbon samples associated with a termination ritual at Structure GZ6.

Guzmán Group

Bayesian model of the Guzmán Group is Figure 5 of the main text. Note that outliers were excluded.

CODE

```
Plot()
 {
  Sequence("Guzmán Group")
  {
   Boundary("Start");
   Phase("The Earliet Occupation")
   {
    R_Date("YU-4695 Plaza Hearth", 1791, 24);
    R_Date("YU-4639 GZ6-Sub 4", 1775, 20);
```

```
};
Boundary("Sealing Chultun 2");
Phase("GZ6 Chultun 2")
{
 R_Combine("C-W Chultun 2")
 {
  R_Date("YU-4131", 1765, 20);
  R_Date("YU-4115", 1757, 20);
  R_Date("YU-4114", 1771, 20);
  R_Date("YU-4088", 1770, 20);
 };
};
Boundary("GZ6-Sub 3");
R_Date("YU-4089 W-Room Floor 4", 1753, 20);
R_Combine("GZ6 E-Room Chultun 3")
{
 R_Date("YU-4133", 1748, 23);
 R_Date("YU-4118", 1733, 21);
};
Boundary("Middle Classic");
R_Date("YU-4134 GZ6-Sub 2", 1613, 20);
Boundary("GZ6-Sub 1");
R_Combine("GZ6 Floor 2")
{
 R_Date("YU-4082", 1570, 20);
 R_Date("YU-4083", 1537, 20);
};
Boundary("Late Classic Early Facet");
Phase("Temple Building")
{
```

```
 R_Date("YU-4101 GZ1-Sub 2 Termination Ritual", 1474, 21);
 R_Combine("GZ3-Sub 1 Chultun 4 Midden")
 {
  R_Date("YU-4682", 1513, 21);
  R_Date("YU-4685", 1486, 21);
  R_Date("YU-4688", 1479, 23);
  R_Date("YU-4693", 1478, 23);
  R_Date("YU-4687", 1477, 20);
  R_Date("YU-4690", 1477, 20);
  R_Date("YU-4694", 1470, 22);
  R_Date("YU-4686", 1454, 20);
  R_Date("YU-4683", 1439, 20);
  R_Date("YU-4692", 1436, 22);
 };
};
Boundary("GZ5-Sub 4 Termination Ritual");
Phase("Plaza")
{
 R_Date("YU-4080 GZ5-Sub 4 Charred Seed", 1332, 20);
 R_Date("YU-4092 Structure GZ6", 1326, 21);
};
Boundary("Structure GZ5-Sub 1");
R_Date("YU-4103 GZ5-Sub 1", 1308, 20);
Boundary("GZ6 Lateral Bench");
R_Date("YU-4106 Burial 2 and Lateral Bench", 1294, 20);
Boundary("Late Classic Late Facet");
Phase("Hieroglyphic Stairway")
{
 Sequence("Building and Use")
 {
```

```
 Phase("Structure GZ1")
 {
  R_Date("YU-4124 Burial 1 Fire Ritual", 1286, 20);
  R_Date("YU-4081", 1279, 20);
  C_Date("Hieroglyphic Stairway", 726, 0);
 };
 Boundary("In Use");
 R_Combine("GZ1 Rituals")
 {
  R_Date("YU-4102", 1259, 20);
  R_Date("YU-4127", 1258, 20);
 };
};
R_Combine("GZ6 Remodeling and Ritual")
{
 R_Date("YU-4085", 1294, 20);
 R_Date("YU-4136", 1284, 20);
 R_Date("YU-4086", 1270, 20);
 R_Date("YU-4105", 1256, 20);
 R_Date("YU-4104", 1250, 20);
};
};
Boundary("Structure GZ3");
Phase("GZ3 Remodeling with Burial 8")
{
 R_Date("YU-4689", 1288, 21);
 R_Date("YU-4684", 1209, 20);
 R_Combine("Fire Ritual")
 {
  R_Date("YU-4678", 1295, 21);
```

```
 R_Date("YU-4677", 1285, 20);
 R_Date("YU-4676", 1270, 22);
 };
};
Boundary("Late-Terminal Classic");
R_Combine("GZ6 Burial 3")
{
 R_Date("YU-4111", 1226, 20);
 R_Date("YU-4108", 1203, 20);
 R_Date("YU-4107", 1201, 20);
};
Boundary("Abandonment");
Phase("Termination Ritual and Abandonment")
{
 R_Date("YU-4638 GZ5", 1214, 20);
 R_Combine("GZ3")
 {
  R_Date("YU-4673", 1223, 21);
  R_Date("YU-4674", 1215, 24);
  R_Date("YU-4641", 1205, 20);
  R_Date("YU-4642", 1198, 20);
  R_Date("YU-4640", 1179, 20);
 };
 R_Date("YU-4125 GZ1", 1205, 20);
 R_Combine("GZ6")
 {
  R_Date("YU-4093", 1226, 20);
  R_Date("YU-4129", 1184, 20);
  R_Date("YU-4128", 1164, 20);
 };
```

```
  };
  Boundary("End");
 };
};
```